

# Towards a high quality in-situ observation network for oxygenated volatile organic compounds (OVOCs) in Europe: transferring traceability to the International System of Units (SI) to the field

Maitane Iturrate-Garcia<sup>1</sup>, Thérèse Salameh<sup>2</sup>, Paul Schlauri<sup>3</sup>, Annarita Baldan<sup>4</sup>, Martin K. Vollmer<sup>3</sup>,  
5 Evdokia Stratigou<sup>2</sup>, Sebastian Dusanter<sup>2</sup>, Jianrong Li<sup>4</sup>, Stefan Persijn<sup>4</sup>, Anja Claude<sup>5</sup>, Rupert Holzinger<sup>6</sup>,  
Christophe Sutour<sup>7</sup>, Tatiana Macé<sup>7</sup>, Yasin Elshorbany<sup>8</sup>, Andreas Ackermann<sup>1</sup>, Céline Pascale<sup>1</sup>, Stefan  
Reimann<sup>3</sup>

<sup>1</sup> Department of Chemical and Biological Metrology, Federal Institute of Metrology (METAS), Bern-Wabern, 3003, Switzerland

10 <sup>2</sup> IMT Nord Europe, Institute Mines-Télécom, Univ. Lille, Centre for Energy and Environment, F-59000 Lille, France

<sup>3</sup> Laboratory for Air Pollution and Environmental Technology, Empa, Swiss Federal Laboratories for Materials Science and Technology, Dübendorf, 8600, Switzerland

<sup>4</sup> VSL-National Metrology Institute, Delft, 2629 JA, the Netherlands

<sup>5</sup> Meteorologisches Observatorium Hohenpeissenberg, Deutscher Wetterdienst (DWD), 82383 Hohenpeissenberg, Germany

15 <sup>6</sup> Institute for Marine and Atmospheric Research, IMAU, Utrecht University, Utrecht, the Netherlands

<sup>7</sup> Department of Gas Metrology, Laboratoire National de Métrologie et d'Essais – LNE, Paris CEDEX 15, 75724, France

<sup>8</sup> School of Geosciences, College of Arts & Sciences, University of South Florida, Florida, USA

*Correspondence to:* Maitane Iturrate-Garcia (maitane.iturrate@metas.ch)

**Abstract.** Volatile organic compounds (VOCs) have a large impact on the oxidising capacity of the troposphere and are major  
20 precursors of tropospheric ozone and secondary atmospheric aerosols. Accurate measurements and data comparability of  
VOCs among monitoring networks are essential to assess the trends of these secondary air pollutants. Metrological traceability  
of the measurements to the international system of units (SI-traceability) contributes to both: measurement consistency and  
data comparability. Accurate, stable and SI-traceable reference gas mixtures (RGMs) and working standards are needed to  
achieve SI-traceability through an unbroken chain of calibrations of the analytical instruments used to monitor VOCs.  
25 However, for many oxygenated VOCs (OVOCs), such RGMs and working standards are not available at atmospheric amount  
of substance fraction levels ( $< 10 \text{ nmol mol}^{-1}$ ). Here, we present the protocols developed to transfer SI-traceability to the field  
by producing two types of SI-traceable working standards for selected OVOCs. These working standards, based on RGMs  
diluted dynamically with dry nitrogen and on certified spiked whole air samples, were then assessed using Thermal Desorption-  
Gas Chromatography-Flame Ionization Detector (TD-GC-FID) and Proton Transfer Reaction-Time of Flight-Mass  
30 Spectrometry (PTR-ToF-MS) as analytical methods. For that purpose, we calibrated five analytical instruments using in-house  
calibration standards and treated the new SI-traceable working standards as samples. Due to analytical limitations, the  
assessment was only possible for acetaldehyde, acetone, methanol and methyl ethyl ketone (MEK). Relative differences  
between assigned and measured values were used to assess the working standards based on dilution of RGMs. The relative  
differences were within the measurement uncertainty for acetone, MEK, methanol and acetaldehyde at amount of substance

35 fractions around  $10 \text{ nmol mol}^{-1}$ . For the working standards based on certified spiked whole air samples in pressurized cylinders, results showed a good agreement among the laboratories (i.e., differences within the measurement expanded uncertainties (U) ranging between  $0.5 \text{ nmol mol}^{-1}$  and  $3.3 \text{ nmol mol}^{-1}$ ) and with the certified amount of substance fraction value for acetaldehyde ( $15.7 \text{ nmol mol}^{-1} \pm 3.6 \text{ (U) nmol mol}^{-1}$ ), acetone ( $17 \text{ nmol mol}^{-1} \pm 1.5 \text{ (U) nmol mol}^{-1}$ ) and MEK ( $12.3 \text{ nmol mol}^{-1} \pm 2.3 \text{ (U) nmol mol}^{-1}$ ). Despite the promising results for the working standards based on the dilution of RGMs and on certified spiked  
40 whole air samples filled into pressurized cylinders, the assessment must be considered with care due to the large measurement uncertainty, particularly for methanol. Active collaboration among metrological, meteorological and atmospheric chemistry monitoring communities is needed to tackle the challenges of OVOC monitoring, such as the lack of stable and SI-traceable calibration standards (i.e., RGMs and working standards). Besides from this collaboration, other research applications, such as modelling and remote sensing, may benefit from the transfer of SI-traceability to monitoring stations.

45

### Keywords

Calibration, metrological traceability, uncertainty, VOCs, tropospheric ozone, reference gas mixtures, GC-FID, PTR-MS

## 1 Introduction

Tropospheric ozone plays a key role in the oxidative capacity of the atmosphere (Iglesias-Suarez et al., 2018; Monks et al.,  
50 2015; Schultz et al., 2015) through different chemical reactions, such as ozone photodissociation, which is the dominant source of hydroxyl radical (OH) in the troposphere (e.g., Lelieveld and Dentener, 2000; Zhang et al., 2014). Besides being a strong oxidant with direct impact on human respiratory health, vegetation growth and crop productivity (Van Dingenen et al., 2009; Schultz et al., 2017; Mills et al., 2018), tropospheric ozone is also a greenhouse gas and a secondary air pollutant (Gaudel et al., 2018; Szopa et al., 2023). In the troposphere, ozone abundance depends on its transport from the stratosphere, formation  
55 and destruction through photochemical reactions and dry deposition (Cooper et al., 2014; Fleming et al., 2018; Jacob, 2000; Stohl et al., 2003; Wild, 2007). Volatile organic compounds (VOCs) – a group of chemical compounds with one or more atoms of carbon and a complex speciation that encompasses thousands of species (Goldstein and Galbally, 2007; Yang et al., 2016) – are one of the major tropospheric ozone precursors (Shao et al., 2009; Xue et al., 2014; Simon et al., 2015). VOC oxidation in the presence of significant amount of substance fractions of nitrogen oxides ( $\text{NO}_x$ ) results in a net production of ozone  
60 (Collins et al., 2002; Pugliese et al., 2014).

Oxygenated VOCs (OVOCs) are an important fraction of VOCs, which includes alcohols, carbonyls (aldehydes and ketones) and carboxylic acid (Legreid et al., 2007; Wu et al., 2020). OVOCs are precursors of tropospheric ozone and secondary organic aerosols and have, thus, an impact on air quality and climate (Boucher et al., 2013; Seinfeld et al., 2016; Shrivasta et al., 2017). OVOCs can be formed by atmospheric photooxidation of hydrocarbons (Atkinson, 2000) and can be emitted directly from  
65 vegetation, biomass burning, vehicle exhaust and industrial processes (Placet, 2000; Legreid et al., 2007; Worton et al., 2022). OVOCs with low molecular weights (e.g., methanol, acetone, acetaldehyde, methyl ethyl ketone (MEK)) are found at relatively

high amount of substance fractions in the global atmosphere and play an important role in the tropospheric photochemistry. For these OVOCs, the main sinks are oxidation with OH radicals and degradation initiated by photolysis leading to the formation of hydrogen oxide radicals ( $\text{HO}_x$ ). For example, oxidation products of methanol are formaldehyde and CO (Bates et al., 2021; Hu et al., 2011), which also impact the oxidation capacity of the troposphere. Acetone, acetaldehyde and MEK are oxidised to peroxy radicals that react with  $\text{NO}_2$  to form peroxyacetyl nitrate (PAN), which is an important precursor of tropospheric ozone (Millet et al., 2010; Fischer et al., 2012; Khan et al., 2015; Wang et al., 2019) and can lead to the transport of radicals and  $\text{NO}_2$  over long distances. Production of radicals (e.g., OH,  $\text{HO}_x$ ) and PAN further affect the chemistry of the tropospheric ozone (Volkamer et al., 2010; Fischer et al., 2014; Tan et al., 2019; Brewer et al., 2020; Zborowska et al., 2021). Therefore, accurate OVOC monitoring is crucial to assess tropospheric ozone burdens, trends and variability.

The Tropospheric Ozone Assessment Report – Phase I (TOAR-I) identified uncertainties associated to ozone precursors' emissions, including VOCs, as one of the main contributors to the uncertainty of modelled spatial and temporal distribution of ozone (Young et al., 2018). Long-term accurate measurements of ozone precursors are required to reduce the uncertainties of their emissions. This need of accurate measurements was also highlighted in TOAR-I as part of the scientific tasks, goals and requirements for tropospheric ozone monitoring (Tarasick et al., 2019). Other programs and infrastructures for atmospheric monitoring emphasise the importance of monitoring VOCs, particularly OVOCs, because of their active role and impact on chemistry of the atmosphere, air quality and climate change. The World Meteorological Organisation Global Atmosphere Watch (WMO-GAW) programme has listed methanol, ethanol, acetone and formaldehyde as part of reactive gas compounds to be monitored (Schultz et al., 2015). The European Aerosol, Clouds and Trace Gases Research Infrastructure (ACTRIS) (Laj et al., 2024) – through its Centre for Reactive Trace Gases In Situ Measurements (CiGas) – includes OVOCs as one of the four compound clusters to be monitored, together with non-methane hydrocarbons, condensable vapours and  $\text{NO}_x$  (Hoerger et al., 2015; Simon et al., 2023). Metrological traceability of the measurements, ideally to the International System of Units (SI), is essential to guarantee data comparability among the different monitoring networks (Brewer et al., 2018; Güttler and Richter, 2009; Worton et al., 2023).

Metrological traceability is achieved through an unbroken chain of calibrations, each contributing to the uncertainty of measurements (De Bièvre and Taylor, 1997). One way of ensuring SI-traceability is to calibrate analytical instruments, which are used to monitor atmospheric compounds, against a primary reference material produced by a National Metrology Institute (NMI). NMIs prepare these materials following reference procedures, provide complete uncertainty budgets of the assigned values, ensure their stability period, and participate in international comparisons with other NMIs to achieve SI-traceability (Brewer et al., 2018). However, for certain reactive compounds, such as many OVOCs (e.g., methanol, ethanol), producing reference material is particularly challenging because of surface, non-linearity and matrix effects, as well as because of stability issues and the low amount of substance fractions (at  $\text{nmol mol}^{-1}$  level) required (Grenfell et al., 2010; Leuenberger et al., 2015; Persijn and Baldan, 2023; Rhoderick et al., 2019).

SI-traceable reference gas mixtures (RGMs) have been developed at NMIs for an increasing number of OVOCs in the last decade (e.g., Brown et al., 2013; Worton et al., 2023). Nevertheless, RGMs are only available at higher amount of substance

fractions than atmospheric ones (Rhoderick et al., 2019; Worton et al., 2022). When monitoring atmospheric OVOCs, these higher amount fractions imply that RGMs must be diluted at monitoring stations before calibrating the analytical instruments. Depending on the dilution procedure, SI-traceability might be lost because of inadequate dilutions (e.g., using dilution devices such as thermal mass flow controllers, whose calibration is not SI-traceable). Another issue faced by OVOC monitoring stations regarding these RGMs is that the matrix gas of the mixture is not the same as ambient air. Quite often, nitrogen is used as matrix gas to ensure the inertness of OVOCs like acetaldehyde. The use of dry nitrogen instead of humidified synthetic air may influence the calibration results. The lack of SI-traceability and long-term stability of OVOC RGMs produced at low amount fraction levels are other limitations that often have negative effects particularly on long-term OVOC measurements. All these aspects have an impact on data comparability and thus on OVOC trend identification.

Here we present the efforts done between the metrological and atmospheric monitoring communities to transfer SI-traceability to the field. For that purpose, protocols to produce two types of SI-traceable working standards – based on dynamic dilution of RGMs with dry nitrogen and on certified spiked whole air samples – of selected OVOCs were developed and assessed. OVOCs were selected in close collaboration with stakeholders (e.g., WMO-GAW, ACTRIS) based on their relevance for atmospheric and climate research, on their role as tropospheric ozone precursors and on the lack of accurate, stable and SI-traceable calibration standards. The selected OVOCs were acetaldehyde, acetone, ethanol, methacrolein, methanol, methyl ethyl ketone (MEK) and methyl vinyl ketone (MVK). The amount of substance fractions of the produced working standards were as close as technically feasible to the ambient air amount of substance fractions ( $< 10 \text{ nmol mol}^{-1}$ ). In this work, we used the quantity amount of substance fraction (a.k.a. amount fraction) – the accepted metrological term (Matschat et al., 2023; Richter, 2007) – instead of concentration and/or mixing ratio. We expressed this quantity in SI units of  $\text{nmol mol}^{-1}$ , which can be considered equivalent to part per billion (ppb) under tropospheric conditions (Galbally et al., 2013).

## **2 Working standards traceable to the international system of units (SI)**

Two types of SI-traceable OVOC working standards were prepared and assessed in this work (Fig. 1): working standards based on the dynamic dilution of SI-traceable reference gas mixtures and working standards based on certified spiked whole air samples. While for the former a dilution step was needed before assessment, the latter was assessed directly without further dilution. The target amount fraction of each OVOC (acetaldehyde, acetone, ethanol, methacrolein, methanol, MEK and MVK) was  $10 \text{ nmol mol}^{-1}$  or lower, to be as close as possible to the OVOC ambient levels. The assessment of the SI-traceable working standards was performed using several analysers based on two analytical techniques (Fig. 1; Appendix A): Thermal Desorption-Gas Chromatography-Flame Ionization Detector (TD-GC-FID) and Proton Transfer Reaction-Time of Flight-Mass Spectrometry (PTR-ToF-MS). The analysers were calibrated with the participants' in-house working standards (Appendix D.1). The SI-traceable working standards were treated as samples.

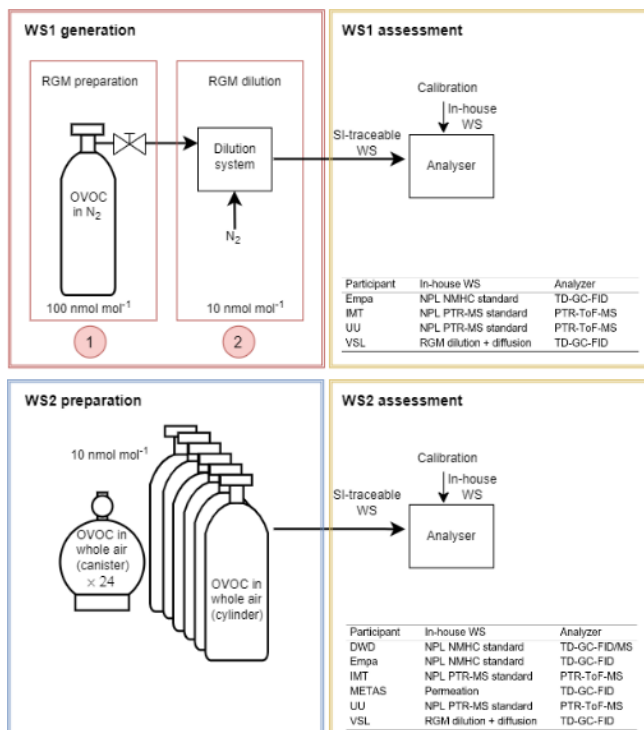


**Figure 1: Scheme showing the two types of working standards traceable to the international system of units (SI) prepared in this work, based on the dilution of reference gas mixtures (RGM) of oxygenated volatile organic compounds (OVOC) in nitrogen (N<sub>2</sub>) (WS1; for details, see section 2.1) and on certified spiked whole air samples (WS2; for details, see section 2.2). Participants in the assessment, analysers (thermal desorption (TD)-gas chromatography (GC)-flame ionization detector (FID) and proton transfer reaction (PTR)-Time of Flight (ToF)-mass spectrometry (MS) systems) and in-house working standards used to calibrate them are indicated.**

## 2.1 Generation of SI-traceable working standards based on dynamic dilution of reference gas mixtures

The first type of SI-traceable working standards developed was based on the dilution of SI-traceable RGMs containing the selected OVOCs at amount fractions of ca. 100 nmol mol<sup>-1</sup>). To achieve the 10 nmol mol<sup>-1</sup> or lower target amount fraction of the SI-traceable working standards dynamic dilution of the produced RGMs was needed (Fig. 1). Dry nitrogen of high purity (≥ 99.99990 %) was used as matrix and dilution gas to prevent any possible reaction (e.g., oxidation) of OVOCs. The potential presence of water and OVOCs in the matrix and the dilution gas was assessed following standard procedures (ISO 19229:2019, 2019).

### 2.1.1 Gravimetric preparation of RGMs

Four RGMs of OVOCs in dry, high-purity (≥ 99.99990 %) nitrogen (BIP+ Built-in-Purifier, Air Products Inc., PA, USA) were prepared at VSL, the National Metrology Institute (NMI) of the Netherlands, in August 2021. For that purpose, the primary gravimetric method was used by means of a high-resolution mass comparator (ISO 6142-1:2015, 2015). In this method, pure

liquid compounds are injected in high-pressure gas cylinders. Prior to the injection, the purity of the selected liquid OVOCs  
150 was analysed (Appendix B.1, Table B1).

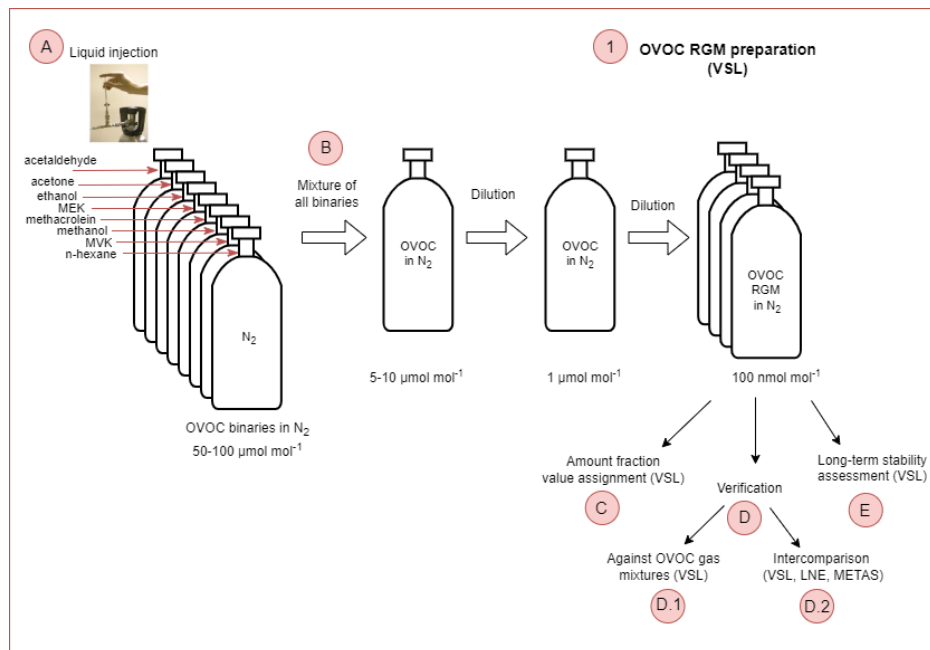


**Figure 2: Schematic diagram illustrating the steps needed to prepare the reference gas mixtures (RGMs) of the selected oxygenated volatile organic compounds (OVOCs).**

### A. Liquid OVOC injection

155 Known amounts of the pure liquid OVOCs were injected in high-pressure gas cylinders to obtain binary gas mixtures at around  $50-100 \mu\text{mol mol}^{-1}$  in a first step (Fig. 2-A). Besides the injected OVOCs, n-hexane was added as internal standard to assess RGM stability (Table B1).

### B. Mixture of binaries and further dilution

160 Then, the binary gas mixtures were combined and further diluted to obtain OVOC RGMs at nominal amount fractions around  $100 \text{ nmol mol}^{-1}$  and at a pressure of 12 MPa (Fig. 2-B). The RGMs were prepared in 10 L aluminium cylinders (Luxfer Inc., CA, USA) with an Experis® proprietary treatment (Air Products Inc., PA, USA) and a low dead-volume stainless steel cylinder valve D304 (Rotarex, Luxemburg).

### C. Amount fraction value assignment

165 RGM amount fraction value assignment was based on gravimetry, with exception of methanol and ethanol. For these compounds, the value was assigned by analysis against dynamically prepared OVOC RGMs. Metrological traceability of the

gravimetric RGMs was ensured by mass weighing and purity determination, while for methanol and ethanol, by mass weighing, volume and purity determination.

## D. Verification

### D.1. Verification against OVOC gas mixtures

170 After preparation (between end of August and mid-September 2021), RGMs were verified against OVOC gas mixtures that contained acetone, ethanol, methacrolein, methanol, MVK and MEK and were generated by a diffusion method (ISO 6145-8:2005, 2005). For acetaldehyde, continuous syringe injection (ISO 6145-4:2004, 2004) and dynamic dilution of a RGM at high amount fraction (ISO 6145-7:2018, 2018) were used. The verification process was performed by VSL (Appendix B.2.1). For each compound, a response factor was calculated according to Eq. (1), which was used to estimate the compound amount  
175 fraction in the gravimetric RGM following Eq. (2). RGM verification was based on the evaluation of the relative difference between the calculated amount fraction and the gravimetric value.

$$RF_i = \frac{(\bar{A}_{cal,i} - \bar{A}_{0i})}{x_{cal,i}} \quad (1)$$

where,

$RF_i$ : compound  $i$  response factor

180  $\bar{A}_{cal,i}$ : average peak area of compound  $i$  in the calibration standard (last five replicates)

$\bar{A}_{0i}$ : average peak area of compound  $i$  in the blanks (last five replicates)

$x_{cal,i}$ : amount fraction of compound  $i$  in the calibration standard

$$x_i = \frac{(\bar{A}_i - \bar{A}_{0i})}{RF_i} \quad (2)$$

185 where,

$x_i$ : estimated amount fraction of compound  $i$  in the sample

$\bar{A}_i$ : average peak area of compound  $i$  in the RGM (last five replicates)

$\bar{A}_{0i}$ : average peak area of compound  $i$  in the blanks (last five replicates)

$RF_i$ : response factor of compound  $i$  calculated according to Eq. (1)

190

### D.2. Interlaboratory comparison

A comparison between three laboratories took place to complete the RGM amount fraction verification. During this interlaboratory comparison (Appendix B.2.2), one of the verified VSL RGMs (VSL221418) was analysed at VSL and at the NMIs of France (LNE) and Switzerland (METAS) between January and April 2022 using the analytical methods described in  
195 Table B3.

## E. Long-term stability assessment

In order to assess the long-term stability of the RGMs, repeated analysis with two to three measurement series were performed 5 months, 7 months, 13 months and 18 months after preparation. Relative differences between averaged measured values for each period and gravimetric values were used as an indicator of temporal stability. The uncertainty of the RGMs, provided together with the assigned value of the amount fraction of each OVOC, was evaluated after the verification and long-term stability assessment. Preparation and verification uncertainty sources were considered to estimate the uncertainty of the RGMs based on the measurement model proposed in ISO 6142-1:2015 (2015). Regarding the preparation sources, uncertainties from weighing, molar masses (Coplen et al., 2020; van der Veen et al., 2021) and the purity of the materials used was propagated using the law of uncertainty propagation (JCGM 100:2008, 2008).

The uncertainty was evaluated using an in-house made software based on the work described in Alink and Van Der Veen (2000). Uncertainty sources linked to RGM verification included the repeatability of each series of measurements and the spread among the series of measurements. A Student's t-test was used to determine whether the mean difference between average analytical observed values and gravimetric values was significant. When significant, the uncertainty due to initial loss was included in the uncertainty evaluation (Eq. (3)).

$$u_c = \frac{1}{2} \cdot \sqrt{u^2(\text{prep}) + u^2(\text{ver}) + u^2(\text{loss})} \quad (3)$$

where,

- $u_c$ : combined uncertainty of the amount fraction of the compound
- $u(\text{prep})$ : gravimetric preparation standard uncertainty
- $u(\text{ver})$ : analytical verification standard uncertainty
- $u(\text{loss})$ : standard uncertainty due to initial loss

An additional term was added to the combined uncertainty of the RGMs sent around for SI-working standard assessment to account for potential temporal instabilities during the shipment period. The expanded uncertainty was then calculated as the combined uncertainty multiplied by the coverage factor ( $k = 2$ ).

### 2.1.2 RGM dilution

SI-traceable working standards containing OVOCs at atmospheric amount fractions ( $10 \text{ nmol mol}^{-1}$ ) were generated by diluting the described RGMs with clean and dry nitrogen using two different dilution systems (Fig. 1). Both dilution systems were warmed up for at least 24 hours and flushed with zero gas (i.e., dry high-purity nitrogen) to prevent presence of water or any other contaminant, before the preparation of working standards. The first dilution system was developed by VSL and consisted of one-stage gas dilution with dilution flows ranging  $2\text{--}50 \text{ L min}^{-1}$ , allowing dilution ratios up to 1:1000 (Appendix A.2). This dilution system was used only during the working standard assessment performed by VSL.



The second dilution system – referred to as "VeRDi" (Versatile Reactive Gas Diluter) and developed by METAS in collaboration with Swagelok® Switzerland – was a two-stage gas diluter allowing dilution ratios up to 1:175000 (Appendix A.2). This dilution system was transferred to the institutes assessing the SI-traceable working standards except to VSL.

## 2.2 Preparation of SI-traceable working standards based on certified spiked whole air samples

The second type of SI-traceable working standards developed consisted of certified whole air samples that were previously spiked with the selected OVOCs to obtain amount fractions around  $10 \text{ nmol mol}^{-1}$ . A schematic of the steps given to prepare these SI-traceable working standards is shown in Figure 3.

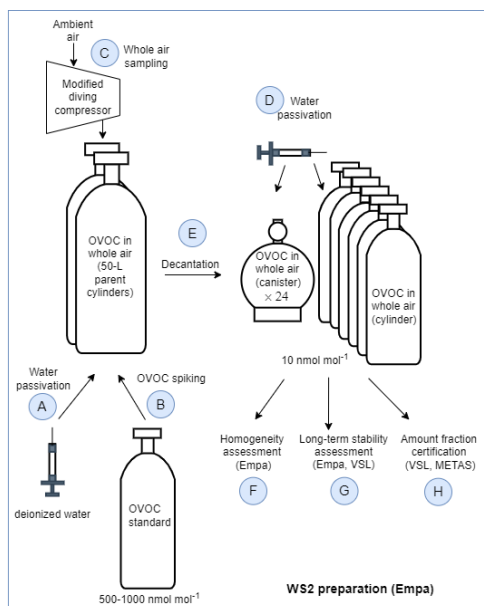


**Figure 3: Schematic diagram illustrating the steps needed to prepare the SI-traceable working standard based on certified spiked whole air samples (WS2).**

240

### A. Water passivation of the parent cylinders

Two 50 L aluminium cylinders (parent cylinders) were selected and filled with ambient air by the Swiss Federal Laboratories for Materials Science and Technology (Empa). Before filling both cylinders were evacuated in parallel for one hour (cylinder pressure  $< 10 \text{ hPa}$ ) with a membrane pump. Then, to passivate their inner walls with a layer of water to reduce adsorption and surface reactions of the compounds of interest, 0.73 mL of deionized water (Merck Millipore, Germany) was injected individually in each parent cylinder at Empa on 31 March 2021.

245

### B. OVOC spiking

OVOC spiking was done using a high-pressure cylinder containing an SI-traceable RGM of OVOCs in dry high-pure nitrogen (VSL, Netherlands) at amount fraction levels between 500 nmol mol<sup>-1</sup> and 1000 nmol mol<sup>-1</sup> (Table C1). This SI-traceable RGM was connected to the parent cylinders via a cross connector and a vacuum pump fitted with an on/off valve to isolate the pump from the cylinders. The spiking took place at Empa three weeks after the water passivation of the parent cylinders. Both water and OVOC spiking were carried out at room temperature.

### 255 **C. Whole air sampling**

One day after the spiking, the two parent cylinders were filled with ambient air at the National Air Pollution Monitoring Network (NABEL) station at "Rigi Seebodenalp" (ca. 1000 m above sea level; Switzerland) on 22 April 2021. The filling was done using a modified diving compressor (RIX Industries, SA-6). The compressor air inlet was about 2 m above ground and placed upwind of the compressor. Both cylinders were filled in parallel during three hours to a final pressure of ca. 145 bar. After the sampling and once back in the laboratory, the parent cylinders were stored tilted (ca. 30° inclination) over night with the top facing downward. Then, the two parent cylinders were taken outdoors and stored for another hour at ambient temperature (10 °C) vertically upside down, before the valves were opened to release the liquid water that was potentially formed during the filling. Since each the spiking and air filling took place with the two parent cylinders connected in parallel, it was assumed that OVOC amount fractions in both cylinders were identical (Table C1).

265

### **D. Water passivation of cylinders and canisters**

Six cylinders and 24 canisters (Table C2) were selected for decanting the parent cylinders to produce several identical subsamples (i.e., working standards). Prior to decanting, the working standard cylinders and canisters were spiked with water – following the same procedure described for the parent cylinders – to achieve a 20 % water saturation level.

270

### **E. Filling of cylinders and canisters (decantation)**

The parent and working standard cylinders, as well as the canisters, were placed in a climate chamber at 40 °C for at least three hours to ensure thermal equilibration before decanting. The interconnecting tubing was kept as short as possible and several tanks of the same type were filled simultaneously. After decanting the parent cylinders, the absolute pressure ranges in the working standard cylinders and canisters were 9.9–10.5 MPa and 0.38–0.41 MPa, respectively. **F. Homogeneity assessment** The homogeneity of the spiked air samples was evaluated before certification (Table C3). For that purpose, seven whole air samples in different vessel types and the two parent cylinders after decantation were analysed three times using Empa GC-FID described in Appendix A.1. The obtained amount fractions were averaged and the variations within the same vessel type and among different vessel types were calculated.

280

### **G. Long-term stability assessment**

Furthermore, during the certification process, the long-term temporal stability of the whole air samples in the cylinders was assessed by repeated measurements after 2 months, 8 months and 14 months. Variations due to temporal instability were included in the certified values.

285

#### H. Certification of the spiked whole air samples

Certification measurements were carried out by VSL and METAS using the two analytical methods described in Table C4 and following the same measurement protocol (Appendix C). Each whole air sample was analysed at least six times. In total, three series of measurements for whole air samples in cylinders were performed, but only one measurement series for the samples in canisters was possible due to the limited sample volume. The amount fraction of each compound per whole air sample was calculated according to Eq. (2). The uncertainty of the assigned amount fraction values included the main uncertainty sources of the sample analysis – such as spread of the analyser response, background noise, blank issues, potential overlapping of GC peaks and detector drift among others – and the uncertainty of the analyser calibration (i.e., uncertainty of the RGMs and possible lack of linearity in the measured range: 0–10 nmol mol<sup>-1</sup>) (Appendix C). The consistency of the assigned amount fraction values for acetone, ethanol, methacrolein, methanol and MVK measured in the same type of vessel was evaluated according to the criterion described by Eq. (4).

290

295

$$|x_{VSL} - x_{METAS}| \leq k \cdot \sqrt{u_{VSL}^2 + u_{METAS}^2} \quad (4)$$

where,

$x_{VSL}$ : amount fraction value of each OVOC under study assigned by VSL

300  $x_{METAS}$ : amount fraction value of each OVOC under study assigned by METAS

$k$ : coverage factor ( $k = 2$ )

$u_{VSL}$ : standard uncertainty of the amount fraction value assigned by VSL according to Eq. (C1)

$u_{METAS}$ : standard uncertainty of the amount fraction value assigned by METAS according to Eq. (C1)

305 Certified reference values for each type of vessel were assigned only when the criterion (Eq. (4)) was met for all OVOCs in the same type of vessel. In this case, the certified reference value of each OVOC was the average of VSL and METAS assigned values for that compound. The relative uncertainty of the certified reference values was the combined uncertainty of the assigned values provided by VSL and METAS, including the spread of the assigned values due to potential temporal instability (one year period).

## 310 4 Assessment of the SI-traceable working standards

### 4.1 Measurement procedure

The SI-traceable working standards were assessed by comparing them against in-house working standards (Appendix D.1), which were used for routine analyser calibrations by the participants in the assessment (Fig. 1): Deutscher Wetterdienst (DWD), Empa, Institute Mines-Télécom (IMT), METAS, Utrecht University (UU) and VSL (Table 2). For that purpose, the  
 315 SI-traceable working standards were treated as samples and analysed following the same procedure as for the analyser calibration. The detailed analytical method, calibration standards and measurement procedure to assess both types of SI-traceable working standards are described in Appendix D.

**Table 2: Information on the assessment of working standards (WS) based on dilution of RGMs with dry nitrogen (WS1) and on certified spiked whole air samples (WS2). ECN refers to the effective carbon number. Detailed information on WS2 samples is shown in Table C2.**

320

| Participant | Dates               | WS  | Samples (assessed WS)  | In-house WS*              | Analytical method |
|-------------|---------------------|-----|--|---------------------------|-------------------|
| IMT         | Jun. 2022           | WS1 | RGM VSL221421 + VeRD <sub>i</sub>  | NPL PTR-MS standard       | PTR-ToF-MS        |
| VSL         | Aug. 2022           | WS1 | RGM VSL221419 + VSL dilutor  | VSL diffusion standard    | TD-GC-FID         |
| UU          | Sep./Oct. 2022      | WS1 | RGM VSL221421 + VeRD <sub>i</sub>  | NPL PTR-MS standard       | PTR-ToF-MS        |
| Empa        | Nov. 2022           | WS1 | RGM VSL221420 + VeRD <sub>i</sub>  | NPL NMHC standard + ECN   | TD-GC-FID         |
| METAS       | Feb. 2022           | WS2 | 001C_cyl, 002A_cyl, 003A_can,<br>004A_can, 004B_can, 005E_can,<br>006B_can, 007A_can, 008A_can | METAS permeation standard | TD-GC-FID         |
| DWD         | Mar. 2022           | WS2 | 001B_cyl, 002B_cyl, 003B_can,<br>005D_can, 008B_can  | NPL NMHC standard         | TD-GC-FID/MS      |
| IMT         | Jun. 2022           | WS2 | 001B_cyl, 002B_cyl, 003B_can,<br>004C_can, 006C_can  | NPL PTR-MS standard       | PTR-ToF-MS        |
| VSL         | Jul. 2021/Aug. 2022 | WS2 | 001A_cyl, 002A_cyl, 003A_can,<br>005B_can, 005C_can, 006D_can,<br>007B_can, 008D_can           | VSL diffusion standard    | TD-GC-FID         |
| UU          | Sep. 2022           | WS2 | 001B_cyl, 002B_cyl, 003B_can,<br>004D_can, 007C_can,   | NPL PTR-MS standard       | PTR-ToF-MS        |
| Empa        | Nov. 2022           | WS2 | 001B_cyl, 002B_cyl, 003B_can,<br>004E_can, 005A_ccan, 006A_can,<br>007D_can, 008C_can          | NPL NMHC standard + ECN   | TD-GC-FID         |

\*All the in-house working standards were SI-traceable except for the effective carbon number (ECN)

To assess the SI-working standards based on certified spiked whole air samples, the same air sample cylinders were measured by the participants in the round-robin comparison (Table 2). However, different canisters were sent to the participants because of the low sample volume, which was enough only for one analysis (Table C2).

## 4.2 Working standard amount fractions and uncertainty

### 4.2.1 Measured amount fractions and uncertainties

The measured amount fractions of the SI-traceable working standards were calculated using different equations depending on the analytical method and the calibration standard used.

VSL estimated the amount fractions of the SI-traceable working standards based on the dilution of RGMs with dry nitrogen according to Eq. (2), using only the last five measurements for the calculations. Uncertainty of these measured amount fractions was calculated following Eq. (C1).

DWD and Empa followed ACTRIS procedures to estimate the OVOC measured amount fractions and their uncertainties (Reimann et al., 2018). The main uncertainty sources considered by DWD and Empa were the reproducibility of the measurement method (i.e., standard deviation of the multiple measurements of the sample) and measurements close to limit of detection, the uncertainty of the in-house working standard (i.e., calibration standard). Sources linked to the uncertainty of the instrument (peak integration uncertainty due to peak overlay, tailing and/or bad peak separation, sampling line artefacts, carry over and changes of split flow rates) were considered in the standard deviation of the multiple calibration measurements. For OVOCs that were not present in the NPL NMHC standard (Grenfell et al., 2010), Empa used the effective carbon number (ECN; e.g., Sternberg et al., 1962; Apel et al., 1998; Faiola et al., 2012). This assessment procedure led to measurement results that are not metrologically traceable. In addition to the sources of uncertainty described above for DWD and Empa, other uncertainties considered in this approach were the mean relative deviation of the NPL NMHC standard certified uncertainties of the six compounds (ethane, ethene, propane, propene, isobutane and butane) contributing to the carbon response factor (CRF) and the relative standard deviation of the six calculated CRFs.

IMT estimated the amount fractions of the selected OVOCs according to the calibration approach described in de Gouw and Warneke (2007). The combined measurement uncertainty,  $u(x_i)$ , was calculated as the square root of the sum of quadrats of each relative uncertainty term (Appendix D.4). Sources of uncertainty associated to the measured amount fractions included precision of the system and calibration accuracy.

UU followed the method described in Holzinger et al. (2019) to estimate the OVOC amount fractions. The uncertainty of the measured amount fractions was given as the standard deviation of 4–6 repetitions of the same measurement type.

#### 4.2.2 Assigned amount fractions and uncertainty

For the SI-traceable working standards based on the dilution of RGMs with dry nitrogen, the assigned amount fraction of each  
355 sample was estimated according to Eq. (5).

$$x_{th} = \frac{(x_{RGM} \cdot q_{v\_RGM} + x_{res} \cdot q_{v\_dil})}{(q_{v\_RGM} + q_{v\_dil})} \quad (5)$$

where,

$x_{th}$ : assigned amount fraction of the generated SI-traceable working standard (in nmol mol<sup>-1</sup>)

$x_{RGM}$ : amount fraction of the OVOC under study in the diluted VSL RGM (in nmol mol<sup>-1</sup>)

360  $x_{res}$ : amount fraction of the OVOC under study present as residual in the dilution gas (in nmol mol<sup>-1</sup>)

$q_{v\_RGM}$ : flow rate of VSL RGM (in mL min<sup>-1</sup>)

$q_{v\_dil}$ : flow rate of the dilution gas (in mL min<sup>-1</sup>)

The uncertainty of the assigned values was calculated following the law of uncertainty propagation (JCGM 100:2008, 2008)  
365 according to Eq. (6). Calculations were done using GUM Workbench Pro version 2.4.1.406 (Metrodata GmbH, Germany).

$$u(x_{th}) = \sqrt{[c_1 \cdot u(x_{RGM})]^2 + [c_2 \cdot u(q_{v\_RGM})]^2 + [c_3 \cdot u(x_{res})]^2 + [c_4 \cdot u(q_{v\_dil})]^2} \quad (6)$$

where,

$u(x_{th})$ : uncertainty of the assigned amount fraction of the generated SI-traceable working standard

370  $u(x_{RGM})$ : uncertainty of the VSL RGM used in the comparison (provided in the calibration certificate according to Eq. (3))

$u(q_{v\_RGM})$ : uncertainty of VSL RGM flow rate

$u(q_{v\_dil})$ : uncertainty of the dilution gas flow rate

$u(x_{res})$ : uncertainty due to the presence of the compound under study in the dilution and matrix gas as impurity

$c_1$ : sensitivity coefficient given by the partial derivative of  $x_{th}$  respect  $x_{RGM}$

375  $c_2$ : sensitivity coefficient given by the partial derivative of  $x_{th}$  respect  $q_{v\_RGM}$

$c_3$ : sensitivity coefficient given by the partial derivative of  $x_{th}$  respect  $x_{res}$

$c_4$ : sensitivity coefficient given by the partial derivative of  $x_{th}$  respect  $q_{v\_dil}$

Assigned amount fractions and uncertainty of the workings standards based on certified spiked whole air samples were  
380 estimated following the procedure described in Appendix C. The relative expanded uncertainty of the certified reference values was two times the combined uncertainty of the assigned values provided by VSL and METAS, including the spread of the assigned values due to potential temporal instability (one year period) (Eq. (C1)).

### 4.2.3 Relative differences between working standards

385 The assessment of the SI-traceable working standards based on the dilution of RGMs with dry nitrogen was done by calculating  
the relative difference between the measured and assigned amount fractions described above, while for the SI-traceable  
working standards based on certified spiked whole air samples, the relative difference between the measured and the certified  
amount fractions was calculated.

390 The expanded uncertainty of each assessment was calculated as two times the combined uncertainty ( $u_{diff}$ ) between the  
uncertainty of the assigned (Table D1) or certified (Table 3) amount fraction ( $u(x_{th})$ ) and the uncertainty of the measured  
amount fraction  $u(x_i)$  reported by the participants (Table D2 and Table D3) for each compound (Eq. (7)).

$$u_{diff} = \sqrt{u^2(x_{th}) + u^2(x_i)} \quad (7)$$

## 395 5 Results

Results regarding the amount fraction assignment and verification of the RGMs used to generate the SI-traceable working  
standards based on the dilution of RGMs and of the assessment of these working standards are shown in this section, together  
with the certification and assessment results of the SI-traceable working standards based on certified spiked whole air samples.

### 5.1 Results of the SI-traceable working standards based on dilution of RGMs

#### 400 5.1.1 RGM amount fraction assignment, verification and stability evaluation

RGM amount fractions were assigned gravimetrically taking into consideration the purity of the liquid chemicals injected into  
the cylinders and results from the mass weighing during the preparation. Results showed purity values > 99.9 % for all the  
liquid compounds, except for methacrolein (98.5 %) and MVK (94.0 %). Water was a common impurity in all the liquid  
compounds. For methacrolein, MVK and MEK, other organic impurities were found (Table B1). Values of the assigned  
405 gravimetric amount fractions ranged between 98 nmol mol<sup>-1</sup> and 105 nmol mol<sup>-1</sup> with expanded uncertainties of the preparation  
≤ 5 % (coverage factor  $k = 2$ ) in general (Table 3). However, greater uncertainties were calculated for methanol (5.3 % in  
VSL221419 and 6.8 % in VSL221420), acetaldehyde (9.6 % in VSL221420 and 9.5 % in VSL221421) and MVK (5.8 % in  
VSL221421) to take into account initial losses and potential instability of these compounds in the cylinders.

410

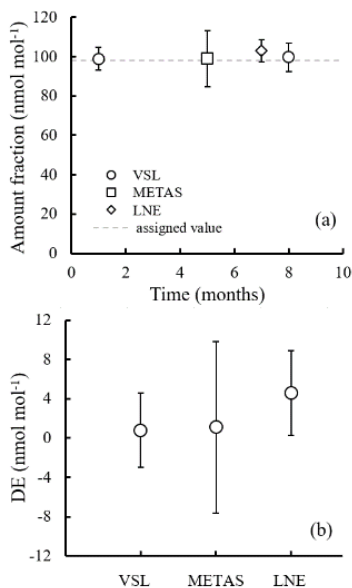
**Table 3: Gravimetric assigned amount fraction values ( $x_i$ ) for the reference gas mixtures (RGMs) and their expanded uncertainty ( $U$ ) with a coverage factor of two ( $k = 2$ )**

| RGM code  | $x_i \pm U$ (nmol mol <sup>-1</sup> ) |            |            |              |             |             |             |
|-----------|---------------------------------------|------------|------------|--------------|-------------|-------------|-------------|
|           | acetaldehyde                          | acetone    | ethanol    | methacrolein | methanol    | MEK         | MVK         |
| VSL221418 | 103.1 ± 2.6                           | 98.1 ± 1.6 | 98.0 ± 2.4 | 100.7 ± 1.6  | 98.0 ± 3.4  | 100.2 ± 1.8 | 101.8 ± 3.0 |
| VSL221419 | 101.9 ± 2.1                           | 99.3 ± 2.2 | 99.2 ± 3.2 | 99.6 ± 2.5   | 99.2 ± 5.3  | 99.1 ± 2.5  | 100.7 ± 4.3 |
| VSL221420 | 103.3 ± 9.6                           | 97.9 ± 4.4 | 93.3 ± 3.8 | 101.0 ± 4.2  | 99.8 ± 6.8  | 100.4 ± 3.9 | 102.1 ± 3.6 |
| VSL221421 | 101.2 ± 9.5                           | 99.9 ± 3.6 | 96.6 ± 5.0 | 99.0 ± 4.1   | 105.1 ± 5.0 | 98.4 ± 3.4  | 100.0 ± 5.8 |

Results from the verification analysis (Table B2), where the prepared RGMs were compared against dynamically generated gas mixtures, showed similar relative differences between analytical and gravimetric values for acetone in the four cylinders (average difference < +0.54 %). These results, similar to the relative differences found for the internal standard (n-hexane), suggest that surface effects (i.e., adsorption losses) were negligible for both compounds. For MEK, the analytical values were also greater than the gravimetric ones and quite similar among different cylinders (average difference < +3.2 %). Lower analytical values than gravimetric ones were found for acetaldehyde, methacrolein and MVK. Average differences were < +2 % and similar among different cylinders for acetaldehyde and methacrolein, which suggests minimal or even negligible adsorption effects with the cylinder wall. The difference was higher for MVK (between -2.5 % and 3.7 %), which might be explained not only by surface effects but also by isomerization reactions. All the relative differences were within the expanded uncertainty of the verification analysis. The relative differences for ethanol were around -5 %. Compound loss after preparation due to surface effects might explain these differences. Initial losses were also suggested by the great heterogeneity among cylinders for methanol (relative difference between -5.2 % and +3.1 %) like described in Persijn and Baldan (2023).

During the interlaboratory comparison organized as part of the RGM verification process (Appendix B.2.2), the three participant laboratories (VSL, METAS and LNE) measured acetone, ethanol and methanol. Results demonstrated a very good comparability and degree of equivalence for acetone (Fig. 4). For methanol, a good agreement among laboratories was also found (Fig. B1), as well as for ethanol. However, due to the great expanded uncertainty (37 %) of the ethanol measurement associated to METAS analytical issues, these results were not considered. It can be noted that although different calibration and analytical methods were used, the measurement results of the RGMS were aligned giving confidence on the quality of the work.





435 **Figure 4: Interlaboratory comparison results for (a) acetone and (b) its degree of equivalence (DE; i.e., the deviation of each laboratory from the reference value). For VSL, only the first measurement period was considered (month 1) to estimate the DE. The measured amount fractions reported by the laboratories were the average of 5 measurements, except for month 1 results, which were the average of 3 measurements. Error bars show the expanded uncertainty of the measurements (coverage factor  $k = 2$ ). The dashed line indicates the gravimetric amount fraction of the compound.**

440 Long-term stability results (Table B4) suggested very good stability (i.e., relative differences between analytical and gravimetric values smaller than  $\pm 5\%$ ) for acetone with relative differences  $\leq +2\%$  even 13–14 months after RGM preparation, although a questionable result ( $-4.7\%$ ) was obtained at a stability testing period of 18–19 months. Acetone results were similar to those for the internal standard (n-hexane). A good stability was also found for methacrolein. After initial relative differences of ca.  $-1.5\%$ , positive values around  $+0.7\%$  were found 7–8 months after preparation. The positive values increased up to

445  $3.4$ – $3.7\%$  during the last stability period (18–19 months). MVK and MEK showed respectively fluctuating positive (up to  $+5.7\%$ ) and negative (up to  $-6.4\%$ ) relative differences most likely due to analytical issues, isomerization reactions and/or surface effects. Ethanol showed a negative relative difference which remained within the  $\pm 5\%$  threshold, except for one of the measurement results obtained at months 18–19 ( $-5.1\%$ ). Acetaldehyde and methanol long-term stability had the largest biases. Varying relative differences  $> \pm 5\%$  (positive for acetaldehyde and negative for methanol) were already found after 5–

450 6 months after preparation, which could be explained by analytical issues, matrix effects and initial compound losses due to adsorption effects.

### 5.1.2 Assessment of SI-traceable working standards based on dilution of RGMs

The assessment of the SI-traceable working standards based on the dilution of RGMs with dry nitrogen took place during a

455 long period of time (ca. six months between the first and last participants). Potential temporal instabilities were considered

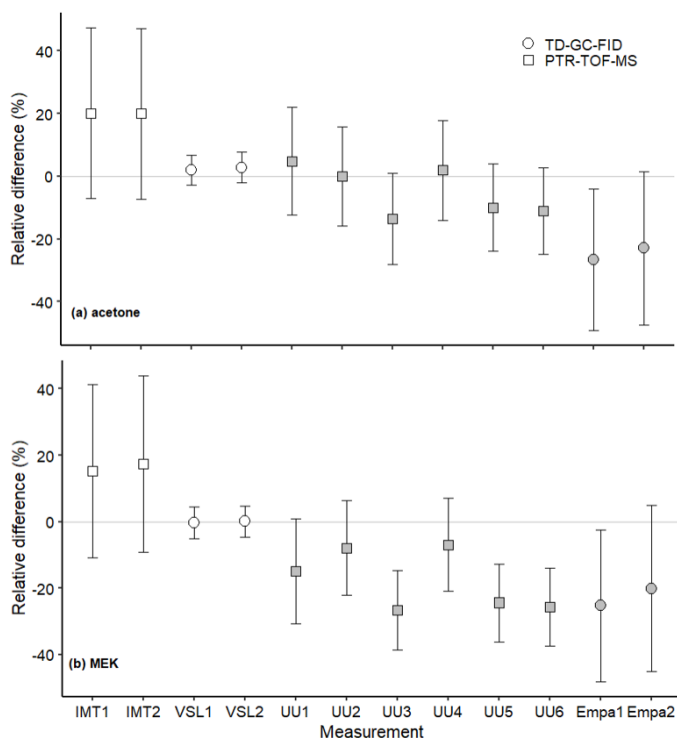
when comparing results through the certified expanded uncertainty provided with the RGMs (Table 3). The long-term RGM stability of each compound was evaluated and taken into account as an uncertainty term (Table B4). The type of in-house standard, sampling method and analytical instrument used, as well as the amount fraction level of the samples generated, were most likely the parameters explaining the differences found between VSL and the other participants for certain compounds, such as MEK (Fig. 5) and methanol (Fig. 6).

Despite relative differences around  $\pm 20\%$  for IMT and Empa, a good agreement between assigned and analytical values (i.e., relative difference around 0 considering the uncertainty of the difference) was found for acetone, even at amount fractions  $< 5 \text{ nmol mol}^{-1}$  (Fig. 5). This agreement demonstrated the reliability of the dilution systems, RGMs and calibration methods. The great relative differences obtained by Empa for acetone were explained by technical issues with the analytical method (i.e., a leak in the heated valve and flow overshooting when measuring with the Stirling cooling unit). The error was estimated to be around  $\pm 30\%$  and was included in the uncertainty budget. These issues also affected Empa MEK and methanol measurements. Therefore, care should be taken in the interpretation of these results.

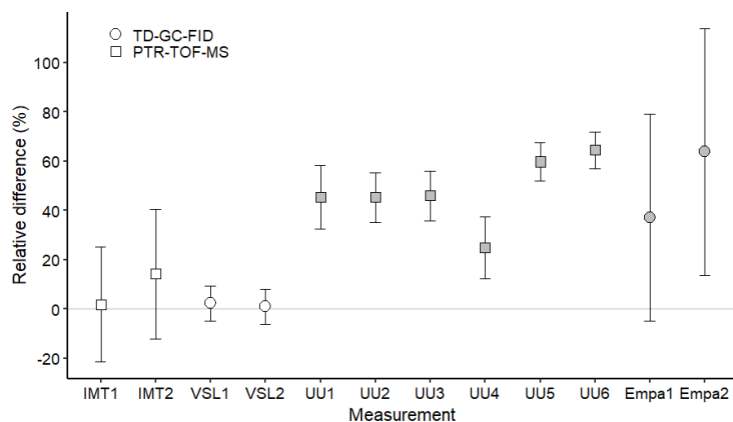
Similar results to acetone working standards were obtained for MEK at amount fractions around  $10 \text{ nmol mol}^{-1}$  (Fig. 5). At lower amount fraction levels ( $< 5 \text{ nmol mol}^{-1}$ ), some of the measurements showed analytical fraction values lower than the assigned ones.

Methanol relative differences were relatively small (1–14 %) and within the uncertainty range at amount fractions between  $10 \text{ nmol mol}^{-1}$  and  $17 \text{ nmol mol}^{-1}$  (Fig. 6). However, at lower amount fractions ( $< 5 \text{ nmol mol}^{-1}$ ) relative differences were between 25–65 %, which suggest an overestimation of the analytical amount fraction values most likely due to artefacts in the analytical system. Moreover, the temporal instability of methanol within the gas cylinder, with an increase in the amount fraction observed during the first year after preparation for one of the RGMs, might contribute to explain part of the overestimation. Methanol instability in gas cylinders was observed in other works (Persijn and Baldan, 2023; Rhoderick et al., 2019). Methanol assessment results suggest, thus, that this OVOC remains a challenging compound to measure.

Acetaldehyde measured and assigned amount fractions showed relatively good agreement, i.e., all the differences were within the uncertainty range (Fig. 7). However, these results must be taken with care because of the large uncertainties. Reactions in the gas cylinders and/or artefacts of the analytical methods might have contributed to analytical amount fractions greater than the theoretical values for acetaldehyde, as well as to uncertainties greater than for the other OVOCs.



485 **Figure 5: Assessment of the SI-traceable working standards based on the dilution of reference gas mixtures with dry nitrogen for (a) acetone and (b) MEK at amount fractions  $< 5 \text{ nmol mol}^{-1}$  (grey symbols) and between 10–17  $\text{nmol mol}^{-1}$  (white symbols). Error bars indicate the expanded uncertainty (coverage factor  $k = 2$ ) of the relative difference between in-house and dilution working standards. Measurement labels show the participant and the number of SI-traceable working standards generated by dilution. Measurements were performed in July 2022 (IMT1, IMT2), August 2022 (VSL1, VSL2), September 2022 (UU1-UU6) and November 2022 (Empa1, Empa2).**



490 **Figure 6: Assessment of the SI-traceable working standards based on the dilution of reference gas mixtures with dry nitrogen for methanol at amount fractions  $< 5 \text{ nmol mol}^{-1}$  (grey symbols) and between 10–17  $\text{nmol mol}^{-1}$  (white symbols). Error bars indicate the expanded uncertainty (coverage factor  $k = 2$ ) of the relative difference between in-house and dilution working standards. Measurement labels show the participant and the number of SI-traceable working standards generated by dilution. Measurements were performed in July 2022 (IMT1, IMT2), August 2022 (VSL1, VSL2), September 2022 (UU1-UU6) and November 2022 (Empa1, Empa2).**

495

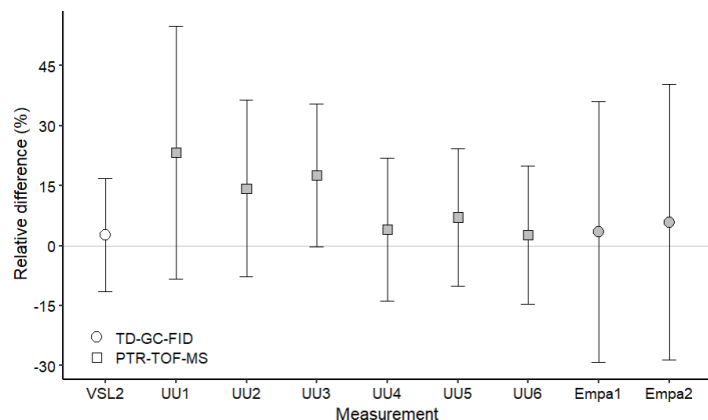


**Figure 7: Assessment of the SI-traceable working standards based on the dilution of reference gas mixtures with dry nitrogen for acetaldehyde at amount fractions  $< 5 \text{ nmol mol}^{-1}$  (grey symbols) and between  $10\text{-}17 \text{ nmol mol}^{-1}$  (white symbols). Error bars indicate the expanded uncertainty (coverage factor  $k = 2$ ) of the relative difference between in-house and dilution working standards. Measurement labels show the participant and the number of SI-traceable working standards generated by dilution. Measurements were performed in August 2022 (VSL2), September 2022 (UU1-UU6) and November 2022 (Empa1, Empa2).**

500

Assessment results for amount fraction levels around  $10 \text{ nmol mol}^{-1}$  suggests that SI-traceable working standards based on dilution of RGMs can be used as calibration standard at monitoring stations for key OVOCs, such as acetone, MEK, methanol and acetaldehyde. However, for lower amount fractions ( $< 5 \text{ nmol mol}^{-1}$ ), suitability of the SI-traceable working standards for MEK, methanol and acetaldehyde is also questionable. The different analytical methods used, the calibration procedure followed and the dilution factors applied to measure and prepare the SI-traceable working standards contributed to that large uncertainty and result dispersion. Further research where the same methodology is followed: same calibration procedure (e.g., same in-house working standard) and assessment protocol (e.g., setting the same dilution factors to generate SI-traceable working standards at the same amount fractions) may reduce both uncertainty and dispersion and help to draw conclusions. Moreover, using coated (e.g., SilcoNert 2000) lines – as short as possible – and low-dead volume pressure reducer, as well as performing long flushing and repeated measurements to guarantee the stability of analyser and dilutor, may reduce the uncertainty of the generated working standards. Even if results are not conclusive, the low RGM uncertainty ( $< 5 \%$ ) and long temporal stability (at least up to 18 months after preparation) are promising to provide atmospheric monitoring stations with SI-traceable accurate OVOC working standards at very low amount fractions.

510

515

## 5.2 Results of the SI-traceable working standards based on certified spiked whole air samples

### 5.2.1 Homogeneity assessment, stability evaluation and amount fraction certification of the spiked whole air samples

Results of the analysis of variance (ANOVA) performed on the data from the homogeneity test of the subset of vessels filled with the spiked whole air samples (Table C3) showed good homogeneity (variation  $< 5 \%$ ) within the same vessel type for all

520

selected OVOCs. The greatest variation was found for methanol (+3.2 %). For the rest of OVOCs, the variation was  $\leq +1.5$  % (e.g., +0.6 % for acetone, +0.9 % for MVK, +1.2 % for MEK and +1.5 % for acetaldehyde and ethanol). Variation among different vessel types suggested that the vessel material may play a role in the lack of homogeneity particularly for methanol (+22.6 %) and ethanol (+9.7 %). Variation was relatively great also for acetaldehyde (+6.6 %), MEK (+6.6 %) and MVK (+7.0 %). However, good homogeneity was found for acetone (+2.8 %) and toluene (+2.4 %). Although toluene is not an OVOC and, thus, was not spiked into the whole air sample vessels, the compound was naturally present in the ambient air.

Temporal stability of the air samples was evaluated by Empa considering the ratio between each OVOC and the internal standard (i.e., n-hexane). Acetone to n-hexane ratios showed good temporal stability (i.e., differences in ratio values among measurements within the uncertainty of the measurement) during the measuring period from August 2021 to September 2022. Except for the uncertainties that were greater, similar results were found for other compounds (methanol, ethanol, acetaldehyde, MVK and MEK). Because the ratio differences observed were within the uncertainty of the measurements and the homogeneity among vessels of the same type was good (variation  $< +2$  % except for methanol (+3.2 %)), air samples in the same type of vessel were considered stable.

Certification results obtained for whole air samples contained in pressurised 10 L aluminium cylinders showed good consistency between the two laboratories performing the certification (i.e., VSL, METAS), with exception of MVK (criterion was not met (Eq. (4)) (Table C5, Figure C1). Regarding the other type of pressurised cylinders (3.6 L stainless steel SilcoNert® coated), the criterion was neither met for MVK. For methanol, the criterion was met only when METAS results were compared against the results obtained for the first measurements performed by VSL (i.e., July 2021). Certified OVOC amount fractions in both cylinders ranged between  $7.6 \text{ nmol mol}^{-1}$  (ethanol) and  $17.3 \text{ nmol mol}^{-1}$  (acetone) with expanded uncertainties ( $k = 2$ )  $\leq 2.6 \text{ nmol mol}^{-1}$  (Table 4). The smallest uncertainties were found for methacrolein and acetone ( $\leq 1.5 \text{ nmol mol}^{-1}$ ). Amount fractions were in line with the estimated spiked values (Table C1) suggesting that, except for acetone, the amount fractions of the selected OVOCs in the sampled air were not significant (close to zero). The higher amount fractions measured for acetone compared to the spiked estimated amount fractions suggested acetone background levels in the sampled whole air of around  $6.5 \text{ nmol mol}^{-1}$ .

Results of the low-pressure canisters were less consistent: the criterion was only met for methacrolein for four canisters (Table C5). For methanol and acetone, the criterion was only met in two canisters. The discrepancy between results for the 15 L canister suggested homogeneity issues for this batch.

**Table 4: Certified amount fraction values ( $x$ ) and their expanded uncertainty ( $U$ ; coverage factor  $k = 2$ ) estimated for the air samples filled in the high-pressure cylinders: 10 L cylinder (MVOC151-001) and 3.6 L (MVOC151-002).**

| compound | $x_{MVOC151-001} \pm U$<br>( $\text{nmol mol}^{-1}$ ) | $x_{MVOC151-002} \pm U$<br>( $\text{nmol mol}^{-1}$ ) |
|----------|---|---|
| methanol | $12.8 \pm 2.0$  | $9.8 \pm 2.5^*$                                       |
| ethanol  | $11.2 \pm 2.6$  | $7.6 \pm 1.9$   |
| acetone  | $17.0 \pm 1.5$  | $17.3 \pm 1.1$  |

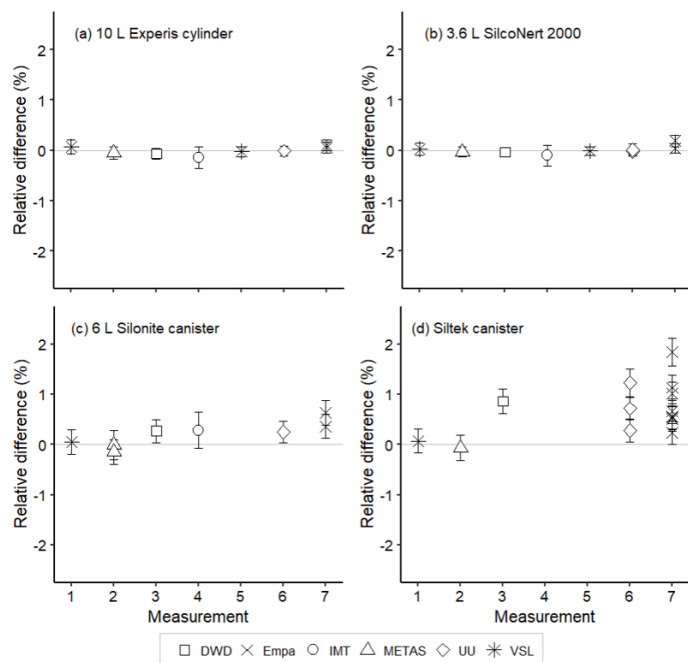
| compound     | $x_{MVOC151-001} \pm U$<br>(nmol mol <sup>-1</sup> ) | $x_{MVOC151-002} \pm U$<br>(nmol mol <sup>-1</sup> ) |
|--------------|--|--|
| methacrolein | 10.7 ± 1.0   | 10.2 ± 0.9   |
| MVK          | 9.4 ± 2.6*   | 8.4 ± 2.3*   |
| MEK          | 12.3 ± 2.3**   | 12.1 ± 2.4**   |

550 \*no compliance with evaluation criterion described in Eq. (4)

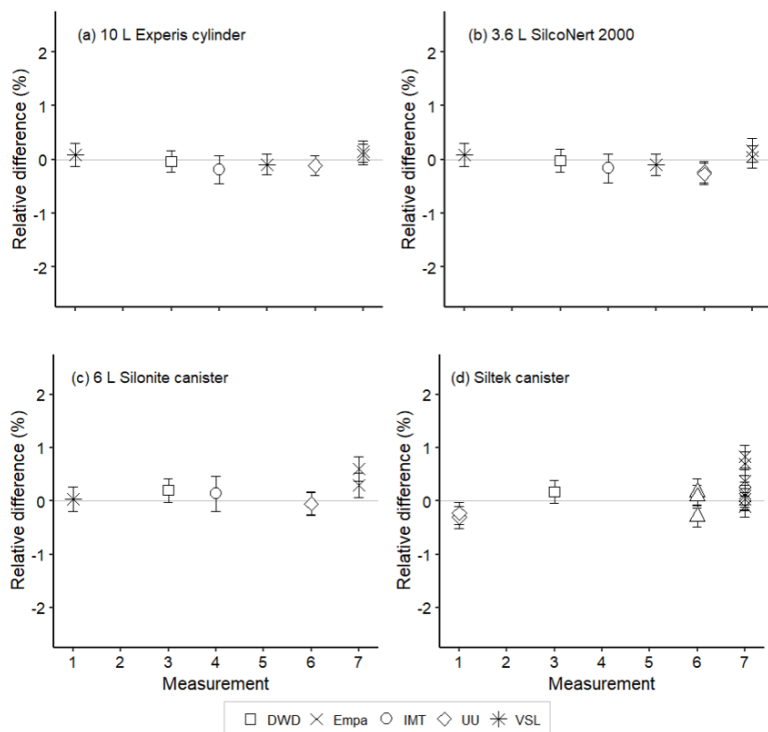
\*\*measurement carried out by only one of the laboratories

### 5.1.2 Assessment of SI-traceable working standards based on certified spiked whole air samples

Amount fractions of the OVOCs measured in air samples showed good agreement (Fig. 8, Fig. 9, Fig. 10) among partners. 555 These values were comparable to the certified amount fractions for whole air samples in cylinders (pressurised at 9.8–10.5 MPa). Only for methanol (Fig. 10), values were more discrepant. Empa results, as for the SI-traceable working standards based on dilution of RGMs with dry nitrogen, must be interpreted with caution because of the technical issues with the analytical system.



560 **Figure 8:** Assessment of the SI-traceable working standards based on certified spiked whole air samples for acetone in (a) 10 L Experis® aluminium cylinders, (b) 3.6 L SilcoNert® 2000 stainless steel cylinders, (c) 6 L Silonite™ stainless steel canisters and (d) 6 L Siltek® stainless steel canisters. Error bars indicate the expanded uncertainty (coverage factor  $k = 2$ ) of the relative difference between the measured and the certified amount fraction values of the working standards. Measurements were performed in Jul. 2021 (1), Feb. 2022 (2), Mar. 2022 (3), Jun. 2022 (4), Aug. 2022 (5), Sep. 2022 (6) and Nov. 2022 (7).



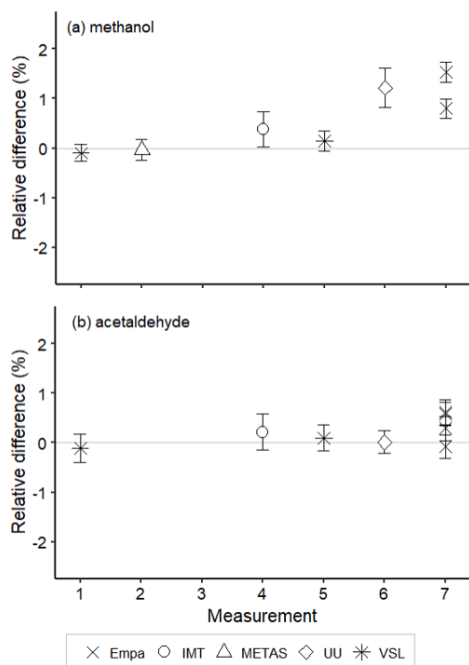
565

**Figure 9: Assessment of the SI-traceable working standards based on certified spiked whole air samples for methyl ethyl ketone (MEK) in (a) 10 L Experis® aluminium cylinders, (b) 3.6 L SilcoNert® 2000 stainless steel cylinders, (c) 6 L Silonite™ stainless steel canisters and (d) 6 L Siltek® stainless steel canisters. Error bars indicate the expanded uncertainty (coverage factor  $k = 2$ ) of the relative difference between the measured and the certified amount fraction values of the working standards. Measurements were performed in Jul. 2021 (1), Feb. 2022 (2), Mar. 2022 (3), Jun. 2022 (4), Aug. 2022 (5), Sep. 2022 (6) and Nov. 2022 (7).**

570

For whole air samples in canisters (pressurised at 0.35 MPa), results were quite heterogeneous. Relatively good results were found for acetone (Fig. 8) and MEK (Fig. 9) in the Silonite™ stainless steel canisters. However, for methanol and acetaldehyde, disagreement was found both among most of the participants and with the certified values. Lack of agreement was also observed for air samples in the Siltek® stainless steel canisters. Even if the same cleaning procedure was followed by both type of canisters before filling, the history (i.e., previous fillings) of the Siltek® stainless steel canisters and/or the surface treatment could explain the differences between canister types. History and surface treatments effects on VOC amount fractions have been reported in previous works (e.g., Rhoderick et al., 2019; Persijn and Baldan, 2023). Furthermore, vessel pressure might explain the differences in result agreement between cylinders and canisters. Gas pressure effects on the stability of gas mixtures in cylinders have been observed for different compounds, such as CO<sub>2</sub> (e.g., Leuenberger et al., 2015; Miller et al., 2015). In these studies, after an initial wall adsorption when the cylinders were filled, desorption took place. This adsorption-desorption process resulted in increasing amount fractions. In Silonite™ canisters, the treatment might have contributed to a lower initial wall adsorption compared to the Siltek® canisters and, therefore, to the lower discrepancies.

580



585 **Figure 10: Assessment of the SI-traceable working standards based on certified spiked whole air samples in 10 L Experis® aluminium cylinders for (a) methanol and (c) acetaldehyde. Error bars indicate the expanded uncertainty (coverage factor  $k = 2$ ) of the relative difference between the measured and the certified amount fraction values of the working standards. Measurements were performed in Jul. 2021 (1), Feb. 2022 (2), Mar. 2022 (3), Jun. 2022 (4), Aug. 2022 (5), Sep. 2022 (6) and Nov. 2022 (7).**

590 Assessment results suggest that certified spiked whole air samples at low amount fractions ( $< 20 \text{ nmol mol}^{-1}$ ) in compressed gas cylinders may be used as SI-traceable working standards for most of the selected OVOCs, except for methanol, at monitoring stations. Using the same matrix gas as the ambient air monitored at atmospheric stations may improve the accuracy of the observations by reducing artefacts and other effects related to the matrix gas.

## 595 **6 Conclusions**

VOCs are one of the major tropospheric ozone precursors. Despite the importance of performing accurate and comparable VOC measurements to assess tropospheric ozone burdens and trends, several challenges regarding VOC monitoring remain currently open. For example, the lack of stable and SI-traceable gas reference materials for many OVOCs at ambient levels and adapted to constraints of monitoring stations (e.g., limited dilution gas supply) among others.

600 This research has shown that producing SI-traceable RGMs at amount fractions around  $100 \text{ nmol mol}^{-1}$ , with expanded uncertainties of the preparation  $< 5 \%$  and temporal stability of at least 14 months, is doable for acetone, methacrolein, MEK, MVK and, to some extent, for ethanol. However, for methanol and acetaldehyde, further research is needed to find suitable



cylinder materials and optimal preparation and analytical procedures (e.g., cylinder wall passivation) to minimize surface adsorption and reaction effects, which greatly contributed to the temporal instability of RGMs for both compounds. These stable and accurate RGMs are produced at amount fraction levels greater than ambient levels of the selected OVOCs (i.e., 4–10 nmol mol<sup>-1</sup>). RGM dilution is thus needed to achieve the amount fraction range required by monitoring stations. To guarantee that SI-traceability is maintained, the dilution needs to be done by a dilution system that is traceable. For that purpose, the elements of the dilution system (e.g., thermal mass flow controller) have to be calibrated against traceable flow standards by NMIs and/or accredited calibration laboratories. Moreover, to reduce as much as possible the uncertainty of the dilution associated to surface effects, the components in contact with the RGM should be coated (e.g., SilcoNert® 2000), low dead-volume pressure reducers should be used and enough time for reaching stability of the dilution and analytical systems should be recommended. The procedure and recommendations described correspond to the SI-traceable working standards based on RGMs diluted with dry nitrogen described in this work, which can be generated at amount fractions around 10 nmol mol<sup>-1</sup> with acceptable relative expanded uncertainties (coverage factor  $k = 2$ ) < 10 % (for acetone and MEK, the expanded uncertainty is even lower than 4 %). This first type of SI-traceable working standard seems to be suitable for calibration of acetone, MEK, methanol and (with larger uncertainties) acetaldehyde at monitoring stations, guaranteeing comparability of the VOC measurements within and among monitoring stations.

Different vessel types were filled with the second type of SI-traceable working standards based on certified whole air samples: high-pressure (> 9.5 MPa) cylinders with different treatments (Experis® and SilcoNert® 2000) and low-pressure (< 0.45 MPa) canisters with two different coatings (Silonite™ and Siltek®). Assessment results suggest that certified spiked whole air samples filled into high-pressure cylinders at amount fractions around 10 nmol mol<sup>-1</sup>, valid for 12–14 months might become a valid alternative for calibrating analytical systems measuring acetone, acetaldehyde and MEK at monitoring stations. Even if VOC RGMs in nitrogen are more stable, this second type of SI-traceable working standard will allow monitoring stations to calibrate their instruments with standards that use similar matrix gas than the ambient air analyzed. Matrix gas effects on the analytical systems are not fully understood yet, but these working standards might provide some insights on the topic. Before going forward with this option, in addition to matrix gas effects on the analytical systems, water passivation and vessel wall effects on the stability of the OVOC amount fractions of these working standards should be explored. Although results of this research suggest that stability might be material dependent, the observed differences might be due to other factors, such as pressure and volume differences among vessels. Specific experiments using new vessels of same volume and pressure (i.e., vessels that were not previously used) should be designed to find the vessel material performing the best.

Despite these promising findings, conclusions must be driven with caution because of the large values and the broad range obtained for the measurement uncertainties (i.e., 5–31 %; coverage factor  $k = 2$ ). Moreover, for both types of working standards, methanol calibration remains challenging.

The RGMs and working standards described in this work are a first step to fulfil the remaining needs of VOC monitoring. Through an active collaboration among metrological, meteorological and atmospheric chemistry monitoring communities, harmonization and comparability among monitoring stations will be promoted (e.g., by estimating uncertainty budgets that are

common to the different monitoring programs). Moreover, this collaboration might provide a better understanding of the impact that pressure, sampling material, moisture and matrix have on the preparation of RGMs and working standards. This knowledge may contribute, thus, to improve calibration standards (i.e., RGMs and SI-traceable working standards) and uncertainties of VOC measurements. Furthermore, other research applications, such as modelling and remote sensing, might benefit from the transfer of SI-traceability to monitoring stations.

## **Appendix A: Analytical instruments and dilution systems**

### **A.1 Analytical instruments**

Thermal Desorption (TD)-Gas Chromatography (GC)-Flame Ionization Detector (FID) and Proton Transfer Reaction (PTR)-Time of Flight (ToF)-Mass Spectrometry (MS) were the two selected analytical methods in this work. The specific analytical instruments used by the laboratories are summarised in Table A1.

#### **DWD (Deutscher Wetterdienst)**

DWD deployed a GC-FID/MS system (6890, 7590 inert XL MS, Agilent Technologies Inc., CA, USA), which was coupled to a custom-made sample pre-concentration unit that included sampling valves, sampling ports and the preconcentration trap in a box heated to 150 °C. Materials in the sampling path were mainly treated stainless steel or capillaries. Samples were preconcentrated on multibed sorbent tubes (Tenax TA 60/80 mesh, Carboxen 602 20/45 mesh and Carboxen 602 20/45 mesh in a ¼" glass tube, Merck KGaA (Supelco), MO, USA) at 30 °C with a sampling flow of 80 mL min<sup>-1</sup>. Desorption to a cryo-focus trap (inert capillary cooled to -180 °C) took place at 200 °C with a flow of 10 mL min<sup>-1</sup>. After heating the cryo-focus to 60 °C, the sample was injected splitless onto a BPX-5 capillary column (50 m length, 0.32 mm internal diameter, 0.5 µm film thickness, Trajan Scientific and Medical (SGE), Australia). The GC oven was held at 13 °C for 18 min. Then, the oven temperature was increased up to 240 °C at a rate of 6 °C min<sup>-1</sup>. Hydrogen (H<sub>2</sub> 5.0 from Air Liquide, France) cleaned using a gas filter (Super Clean gas filter, Restek, PA, USA) was used as a carrier gas at 3.5 mL min<sup>-1</sup>. Subsequent to the separation on the column, the carrier gas flow was split onto the MS and the FID in parallel. For the analysis of the SI-traceable working standards based on spiked whole air, the MS detector was used to achieve sufficient peak separation.

#### **Empa (Swiss Federal Laboratories for Materials Science and Technology)**

Empa used a GC-FID (7890, Agilent Technologies Inc., CA, USA) coupled to a thermal desorber UNITY<sup>TM</sup>-xr (Markes International Ltd., UK) to evaluate the stability and homogeneity of the air samples and to assess the SI-traceable OVOC working standards (Table A1). Samples went through an in-house dehumidifier – consisting of a Stirling cooler (set to -42 °C) and two insulated in-line glass fingers – before sampling, which was done using a UNITY<sup>TM</sup>-Air Server (Markes International Ltd., UK) equipped with three ports. From UNITY<sup>TM</sup>-Air server, samples passed to the thermal desorber, which collected and concentrated the OVOCs under study. The UNITY cold trap (ozone precursors cold trap, U-T1703P-S2; Markes International

Ltd., UK) temperature was set to -29 °C before the cold trap was heated up to 250 °C. The two capillary columns were  
670 OxyPLOT (30 m length, 0.53 mm internal diameter and 10 µm film thickness; Agilent Technologies Inc., CA, USA) and  
Al<sub>2</sub>O<sub>3</sub> HP-PLOT (50 m length, 0.53 mm internal diameter and 10 µm film thickness; Agilent Technologies Inc., CA, USA).  
Sample flow was set at 15 mL min<sup>-1</sup> during 20 min. The GC oven was held at 40 °C for 3.25 min and then heated up to 200  
°C with a temperature ramp of 7 °C min<sup>-1</sup>. The GC oven was held at 200 °C for 20 min. The carrier gas was helium, which  
was set at 5 mL min<sup>-1</sup> for 20 min and then increased at 25 mL min<sup>-1</sup> for 26 min.

675

#### **IMT (Institute Mines-Télécom)**

IMT performed the assessment of SI-traceable working standards using a second generation PTR-ToF-MS (Kore Technology  
Ltd., UK) (Table A1). Sampling was done through a SilcoNert® 1000 heated line at a flow rate of 200 mL min<sup>-1</sup>. An in-house  
system of solenoid valves was coupled to the PTR-ToF-MS to switch automatically between samples and zero air.  
680 Measurement time resolution was set to 10 seconds.

#### **LNE (Laboratoire National de Metrologie et d'Essais; National Metrology Institute (NMI) of France)**

LNE used a GC-FID (7890, Agilent Technologies Inc., CA, USA), equipped with an on-column pre-concentration system,  
during the OVOC RGM comparison (Table A1). The selected capillary column was HP-Plot-U (30 m length, 0.53 mm internal  
685 diameter and 20 µm film thickness; Agilent Technologies Inc., CA, USA). The GC oven was held at a constant temperature  
of 150 °C. The carrier was helium BIP® (Air Products and Chemicals, PA, USA). The sampling was done using a coated  
(SilcoNert® 2000) sample loop, which injected a sample volume of 60 mL. The pre-concentration system was cooled down  
to -60 °C by a liquid nitrogen cryo trap system (JAS 66601 CryoTrap, Joint Analytical Systems GmbH, Germany), which was  
heated up to 150 °C for final injection.

690

#### **METAS (Federal National Metrology Institute; NMI of Switzerland)**

METAS used a GC-FID Clarus 500 (PerkinElmer Inc., MA, USA) coupled to a thermal desorber TurboMatrix 350  
(PerkinElmer Inc., MA, USA) (Table A1). The capillary column was DuraBond DB-624 (30 m length, 0.32 mm internal  
diameter and 1.8 µm film thickness; Agilent Technologies Inc., CA, USA). The carrier gas was helium. The system had a  
695 Tenax-TA sorbent cold trap (Perkin Elmer Inc., MA, USA), which was cooled at -30 °C and heated up to 280 °C at a  
temperature rate of 40 °C s<sup>-1</sup>. The GC oven was held at 40 °C for 2 min and then heated up to 200 °C at 5 °C min<sup>-1</sup>. The GC  
oven was held at 200 °C for 2 min. The sampling was done using conditions multibed sorbent tubes: Carbograph 2TD (mesh  
60/80) – Carbograph 1TD (mesh 40/60) – Carbosieve™ SIII (mesh 60/80) (Camsco, TX, USA). Loading of the sorbent tubes  
were done by means of an in-house loading system at loading volumes between 300 mL (10 min at 30 mL min<sup>-1</sup>) and 450 mL  
700 (15 min at 30 mL min<sup>-1</sup>).

#### **UU (Utrecht University)**

UU used a PTR-ToF-MS with hexapole and ion funnel (PTR-TOF4000, Ionicon Analytik GmbH, Austria) to assess the SI-traceable working standards (Table A1). A SulfiNert® coated 4-port valve (VICI® Valco Instruments Co. Inc., TX, USA) kept at 120 °C was used to switch between zero air and sample inlet. Samples were connected to a PEEK capillary that, depending on the pressure in cylinders and canisters, produced a flow between 80 mL min<sup>-1</sup> and 300 mL min<sup>-1</sup>.

### VSL (NMI of the Netherlands)

VSL used TRACE™ GC (Thermo Fisher Scientific Inc., PA, USA) coupled to a thermal desorber UNITY™ 2 (Markes International Ltd., UK) during the OVOC comparison, the certification of air samples and the assessment of SI-traceable working standards (Table A1). A Deans switch in the GC sent the gas sample to two FID detectors and two capillary columns: Stabilwax (30 m length, 0.32 mm internal diameter and 1.0 µm film thickness; Restek Corporation, PA, USA) for MVK and PoraBOND U (25 m length, 0.32 mm internal diameter and 7 µm film thickness; Agilent Technologies Inc., CA, USA) for the other OVOCs. The cold trap filled with multi-bed sorbent trap (Air Toxics, Markes International Ltd., UK) was cooled down to -20 °C and heated up to 300 °C. Sampling flow was set at 20 mL min<sup>-1</sup> during 30 min. The GC oven was held at 40 °C for 2 min and then heated up to 230 °C with three temperature ramps of 20 °C min<sup>-1</sup> (up to 120 °C), 5 °C min<sup>-1</sup> (up to 180 °C) and 10 °C min<sup>-1</sup> (up to 230 °C). The GC oven was held at 200 °C for 20 min. The carrier gas was helium.

**Table A1: Information on the analytical instruments used in this work.**

| Lab   | Measurements   | Analytical method | Analytical instrument  |
|-------|--|-------------------|--|
| DWD   | Assessment <sup>2</sup>                              | TD-GC-FID/MS      | 6890 GC-FID (Agilent), 7590 inter XL MS (Agilent)<br>Custom made TD unit (DWD) |
| Empa  | Assessment <sup>1,2</sup>                            | TD-GC-FID         | 7890 GC-FID (Agilent)<br>TD UNITY™-xr (Markes International)                   |
| IMT   | Assessment <sup>1,2</sup>                            | PTR-ToF-MS        | second-generation PTR-ToF-MS (Kore Technology)                                 |
| LNE   | Comparison   | TD-GC-FID         | 7890 GC-FID (Agilent)  |
| METAS | Comparison, certification                            | TD-GC-FID         | Clarus 500 GC-FID (Perkin Elmer)<br>TD TurboMatrix 350 (Perkin Elmer)          |
| UU    | Assessment <sup>1,2</sup>                            | PTR-ToF-MS        | PTR-TOF4000 (Ionicon Analytik)   |
| VSL   | Comparison, certification, assessment <sup>1,2</sup> | TD-GC-FID         | Thermo Trace GC-FID;<br>TD UNITY™ 2 (Markes International)                     |

<sup>1</sup>Assessment SI-traceable working standards based on dilution of Reference Gas Mixtures (RGMs) with dry nitrogen

## A.2 Dilution systems

Two dilution systems were used to generate the SI-traceable working standards based on the dynamic dilution of RGMs.

725 The first system, developed by VSL, was a one-stage gas dilutor with dilution flows ranging 2–50 L min<sup>-1</sup>, allowing dilution ratios up to 1:1000. Flows of the RGM (0.1 L min<sup>-1</sup>) and of the dilution gas (nitrogen, AP BIP Plus grade 6.0) were accurately controlled using three MFCs (EL-FLOW® Select series, Bronkhorst, Netherlands), operating up to 10 L min<sup>-1</sup> and 25 L min<sup>-1</sup>. The dilution system was mostly built in inert glass. Other materials in contact with the OVOC gas mixtures were polytetrafluoroethylene (PTFE), 316 stainless steel (SS) (small surfaces) or coated 316 SS (SilcoNert® 2000, SilcoTek, PA, USA). A coated (SilcoNert® 2000) pressure reducer was connected to the RGMs and flushed thoroughly before attaching it to the dilution system. For the purpose of this assessment, the MFCs were set and calibrated using two mercury piston prover volumeters (Bronkhorst, Netherlands), which were in turn calibrated at the VSL Flow Department, at working ranges of 0–0.5 L min<sup>-1</sup> and 0–10 L min<sup>-1</sup>. Temperature and pressure were measured by equipment calibrated at the VSL Temperature and Pressure Department to convert flow to standard temperature and pressure (STP) conditions (293.15 K, 101.3 kPa).

735 The second system ("VeRDi" (Versatile Reactive Gas Diluter)), developed by METAS in collaboration with Swagelok® Switzerland, was a two-stage gas dilution system allowing dilution ratios up to 1:175000. The main components of this dilution system were four MFCs (two MFCs up to 0.1 L min<sup>-1</sup> (Red-y, Vögtlin Instruments, GmbH, Switzerland) and two MFCs up to 5 L min<sup>-1</sup> (Sensirion AG, Switzerland)), two pressure controllers (Bronkhorst High-Tech B.V., Netherlands), a valve terminal (MPA-L, Festo Beteiligungen GmbH & Co. KG, Germany) and a vacuum pump. Elements in contact with RGM flow were coated (SilcoNert® 2000), including all the stainless steel tubing of ¼" internal diameter used to build VeRDi. The tubes were welded, instead of joined through fittings, in order to reduce dead volumes and potential leaks. MFCs and pressure regulators were calibrated using clean and dry nitrogen against METAS primary standards to ensure traceability of the dilution. The software controlling VeRDi was developed in LabVIEW (National Instruments, Austin, TX).

## 745 Appendix B: Purity analysis, stability evaluation and verification of the Reference Gas Mixtures (RGMs)

### B.1 Purity analysis

Prior to their injection in the pressurised cylinders, the pure liquid oxygenated volatile organic compounds (OVOCs), selected to prepare the gravimetric RGMs, were analysed to determine their purity according ISO 19229:2019 (2019). For that purpose, VSL (the national metrology institute (NMI) of the Netherlands) used a gas chromatographic (GC) system (6890, Agilent Technologies Inc., CA, USA) with a mass spectrometer (MS) and a flame ionization detector (FID) equipped with a GS-

GASPRO capillary column (60 m length, 0.32 mm internal diameter and 0.25  $\mu\text{m}$  film thickness; Agilent Technologies Inc., CA, USA). For acetaldehyde, it was not possible to perform the purity analysis because of the physical properties of the liquid chemical, which made its handling difficult. The water content in the liquid OVOCs was determined by the Karl Fischer titration (Coulometric KF titrator, Metrohm). Results of the purity analysis are included in Table B1.

755 **Table B1: Purity of the liquid OVOCs used to prepare the gravimetric reference gas mixtures including the amount fraction of compounds and impurities ( $x_i$ ) and its expanded uncertainty ( $U(x_i)$ ; coverage factor  $k = 2$ ). CAS refers to the chemical abstract service registry number. The purity analysis of acetaldehyde was not possible because of handling difficulties associated to the physical properties of the liquid chemical.**

| Liquid chemical           | CAS      | Supplier                                | Compound   | $x_i$<br>(mol mol <sup>-1</sup> ) | $U(x_i)$<br>(mol mol <sup>-1</sup> ) |
|---------------------------|----------|---|--|-----------------------------------|--------------------------------------|
| acetaldehyde              | 75-07-0  | Acros Organics™, PA, USA                | acetaldehyde   | 0.999 <sup>1)</sup>               | NA                                   |
| acetone                   | 67-64-1  | Sigma-Aldrich®, MA, USA                 | acetone  | 0.999380                          | 0.000124                             |
|                           |          |   | water  | 0.000620                          | 0.000124                             |
| ethanol                   | 64-17-5  | Merck KGaA, Germany                     | ethanol  | 0.999733                          | 0.000054                             |
|                           |          |   | water  | 0.000267                          | 0.000054                             |
| methacrolein              | 78-85-3  | Thermo Fischer Scientific Inc., PA, USA | methacrolein   | 0.985646                          | 0.001683                             |
|                           |          |   | methylal   | 0.003458                          | 0.000692                             |
|                           |          |   | 1,1-dimethoxy-2-butene                               | 0.003600                          | 0.000720                             |
|                           |          |   | hydroquinone   | 0.001000                          | 0.000500                             |
|                           |          |   | water  | 0.006296                          | 0.001260                             |
| methanol                  | 67-56-1  | Sigma-Aldrich®, MA, USA                 | methanol   | 0.999724                          | 0.000056                             |
|                           |          |   | water  | 0.000276                          | 0.000056                             |
| methyl ethyl ketone (MEK) | 78-93-3  | Acros Organics™, PA, USA                | MEK  | 0.999297                          | 0.000147                             |
|                           |          |   | 2,4-dimethyl-hexane <sup>2)</sup>                    | 0.000234                          | 0.000118                             |
|                           |          |   | trichlorodocosyl-silane <sup>3)</sup>                | 0.000037                          | 0.000019                             |
|                           |          |   | water  | 0.000431                          | 0.000087                             |
| methyl vinyl ketone (MVK) | 78-94-4  | Acros Organics™, PA, USA                | MVK  | 0.940938                          | 0.005352                             |
|                           |          |   | Acetonitrile   | 0.008389                          | 0.001678                             |
|                           |          |   | 4-(acetyloxy)-2-butanone                             | 0.006077                          | 0.001216                             |
|                           |          |   | 2-acetyl-5-methyl-2,3-dihydro-4H-pyran <sup>4)</sup> | 0.020687                          | 0.002069                             |
|                           |          |   | p-benzoquinone                                       | 0.001564                          | 0.000313                             |
|                           |          |   | water  | 0.022346                          | 0.004470                             |
| n-Hexane                  | 110-54-3 | Merck KGaA, Germany                     | n-hexane   | 0.991224                          | 0.001307                             |
|                           |          |   | 3-methyl-pentane                                     | 0.002943                          | 0.000589                             |

| Liquid chemical | CAS | Supplier | Compound            | $x_i$<br>(mol mol <sup>-1</sup> ) | $U(x_i)$<br>(mol mol <sup>-1</sup> ) |
|-----------------|-----|----------|---------------------|-----------------------------------|--------------------------------------|
|                 |     |          | methyl-cyclopentane | 0.005831                          | 0.001167                             |
|                 |     |          | water               | 0.000002                          | 0.000001                             |

<sup>1)</sup>Purity value provided by the manufacturer

760 <sup>2)</sup>According to MS database, the first hit with highest probability is 2,4-dimethyl-hexane, but the probability is only around 10 %.

<sup>3)</sup>According to MS database, the first hit with highest probability is trichlorodocosyl-silane, but the probability is only around 15 %.

<sup>4)</sup>The impurity might also be MVK dimer.

## B.2 RGM verification

### 765 B.2.1 Verification measurement results

The verification process was repeated three times using VSL thermal desorption (TD)-GC-FID described in Appendix A.1. The RGMs were connected to an autosampler built by VSL, sharing therefore the same pressure reducer. Lines and pressure reducer were coated (SilcoNert® 2000). To guarantee the same sampling conditions (20 mL min<sup>-1</sup> sampling flow during 15 minutes, total volume 300 mL at 293 K and 101.3 kPa) for gravimetric and dynamically prepared RGMs, the mass flow controller (MFC) of the thermal desorber was operated in light vacuum mode by means of a pump. Each gas mixture was analysed 20 times. Results of the verification measurements performed one month after preparation of the RGMs, estimated according Eq. (2), are shown in Table B2. Three verification measurements were carried out for each RGM.

775 **Table B2: Verification results obtained one month after preparation of the Reference Gas Mixtures (RGMs) gravimetrically prepared RGMs at the National Metrology Institute of the Netherlands (VSL). Three verification measurements (M1, M2 and M3) of the amount fraction of each compound ( $x_i$ ) were performed per RGM. The relative standard deviation (RSD) and the relative difference between analytical and gravimetric values ( $\Delta$ ) are also shown. NA indicates not available data due to an analytical issue during a measurement.**

| Compound     | RGM code  | $x_{i,M1}$<br>(nmol mol <sup>-1</sup> ) | $x_{i,M2}$<br>(nmol mol <sup>-1</sup> ) | $x_{i,M3}$<br>(nmol mol <sup>-1</sup> ) | RSD<br>(%) | $\Delta$<br>(%) |
|--------------|-----------|---|---|---|------------|-----------------|
| acetaldehyde | VSL221418 | 101                                     | 102                                     | 99.2                                    | 1.40       | -2.24           |
|              | VSL221419 | NA                                      | 101                                     | 102                                     | 1.61       | -1.48           |
|              | VSL221420 | 99.0                                    | 102                                     | 102                                     | 1.78       | -2.22           |
|              | VSL221421 | 95.5                                    | 97.6                                    | 106                                     | 5.68       | -1.47           |
| acetone      | VSL221418 | 98.7                                    | 99.4                                    | 98.9                                    | 0.37       | 0.90            |
|              | VSL221419 | NA                                      | 98.9                                    | 101                                     | 1.03       | 0.41            |
|              | VSL221420 | 98.4                                    | 97.4                                    | 99.5                                    | 1.10       | 0.53            |
|              | VSL221421 | 100                                     | 101                                     | 99.7                                    | 0.53       | 0.33            |
| ethanol      | VSL221418 | 97.6                                    | 95.8                                    | 95.5                                    | 1.19       | -1.75           |
|              | VSL221419 | NA                                      | 95.7                                    | 98.7                                    | 5.90       | -5.12           |
|              | VSL221420 | 93.3                                    | 91.0                                    | 93.8                                    | 1.57       | -5.26           |
|              | VSL221421 | 96.6                                    | 97.8                                    | 90.8                                    | 3.93       | -4.75           |

| Compound                     | RGM code  | $x_{i,M1}$<br>(nmol mol <sup>-1</sup> ) | $x_{i,M2}$<br>(nmol mol <sup>-1</sup> ) | $x_{i,M3}$<br>(nmol mol <sup>-1</sup> ) | RSD<br>(%) | $\Delta$<br>(%) |
|------------------------------|-----------|---|---|---|------------|-----------------|
| methacrolein                 | VSL221418 | 98.9                                    | 99.8                                    | 99.6                                    | 0.48       | -1.29           |
|                              | VSL221419 | NA                                      | 97.0                                    | 99.4                                    | 1.23       | -1.62           |
|                              | VSL221420 | 99.2                                    | 98.4                                    | 101                                     | 1.29       | -1.47           |
|                              | VSL221421 | 97.0                                    | 97.7                                    | 99.1                                    | 1.08       | -1.05           |
| methanol                     | VSL221418 | 103                                     | 98.8                                    | 97.6                                    | 2.77       | 1.78            |
|                              | VSL221419 | NA                                      | 96.7                                    | 102                                     | 10.2       | -5.21           |
|                              | VSL221420 | 93.5                                    | 98.1                                    | 101                                     | 4.08       | -0.14           |
|                              | VSL221421 | 106                                     | 105                                     | 98.2                                    | 4.00       | 3.11            |
| methyl ethyl<br>ketone (MEK) | VSL221418 | 103                                     | 104                                     | 103                                     | 0.64       | 3.29            |
|                              | VSL221419 | NA                                      | 101                                     | 103                                     | 0.80       | 2.91            |
| methyl vinyl<br>ketone (MVK) | VSL221420 | 103                                     | 103                                     | 104                                     | 0.78       | 3.07            |
|                              | VSL221421 | 101                                     | 102                                     | 102                                     | 0.42       | 3.21            |
|                              | VSL221418 | 99.0                                    | 99.2                                    | 99.1                                    | 0.11       | -2.66           |
| methyl vinyl<br>ketone (MVK) | VSL221419 | NA                                      | 96.3                                    | 98.5                                    | 1.40       | -3.71           |
|                              | VSL221420 | 99.0                                    | 97.4                                    | 99.1                                    | 0.99       | -3.50           |
|                              | VSL221421 | 95.6                                    | 97.7                                    | 99.3                                    | 1.93       | -2.48           |

### B.2.2 RGM interlaboratory comparison

780 The National Metrology Institutes (NMIs) of France (LNE), Switzerland (METAS) and the Netherlands VSL took part in an interlaboratory comparison to verify the produced RGMs. Three different Thermal Desorption-Gas Chromatography-Flame Ionization Detector (TD-GC-FID) systems and calibration methods (Table B3) were used to analyse the amount fraction of acetone, ethanol and methanol in the RGM sent around (VSL221418).

785 The same coated (SilcoNert® 2000) pressure reducer (RX 2400, Rotarex, Luxemburg) and line (1/16" coated line of 1 m length) were used, for at least one series measurements, by LNE and METAS. VSL used an autosampler (VSL spin) equipped with a multi-position valve (VICI AG International, Switzerland), a coated (SilcoNert® 2000) pressure reducer (Tescom, TX, USA) and coated lines (SilcoNert® 2000, 1/16" diameter, ca. 1 m length). Five series of measurements were performed by LNE and by METAS. VSL performed three series of measurements before shipping the comparison standard to the other laboratories (September 2021) and five series of measurements after the shipment (April 2022). At least five replicates per series were analysed. Individual measurement sequences consisted in the analysis of blank samples (at the beginning and end of each measurement), calibration standard samples (at two amount fraction levels) and comparison standard samples, which were (analysed between the calibration standards to minimise drift effects and prevent biases). LNE sampling was done through a coated (SilcoNert® 2000) sample loop of 20 mL volume; total sample volume was 60 mL. VSL sampling was done by means of the autosampler (Unity 2, Markes International, Ltd., UK) coupled to the TD-GC-FID at a sampling flow rate of 20 mL

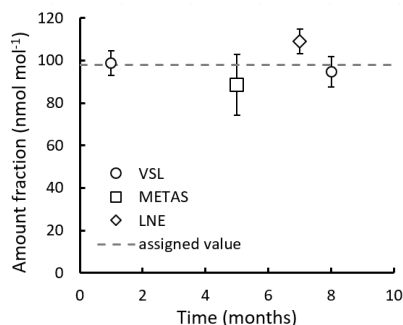


795 min<sup>-1</sup> during 15 minutes (300 mL sample volume). Multibed sorbent tubes (Carbograph 2 (mesh 60/80) – Carbograph 1 (mesh 40/60) – Carbosieve™ SIII (mesh 60/80); Camsco, TX, USA) were used for sampling by METAS; loading volume ranged between 150 mL and 450 mL.

Amount fraction values of the comparison standard were assigned applying Eq. (1) and Eq. (2). Following standard procedures used in key comparisons, the degree of equivalence of each laboratory for acetone was estimated as the difference  
800 between analytical measurement values obtained by each laboratory and the gravimetric reference value provided by VSL.

**Table B3: Information on the interlaboratory comparison measurements of one of the OVOC reference gas mixtures (RGMs; VSL221418) prepared by VSL to generate SI-traceable working standards based on its dilution using dry nitrogen.**

| Lab   | Date                       | Analytical instrument  | Capillary column (length, internal diameter, film thickness) | Calibration method                 |
|-------|----------------------------|--|--|------------------------------------|
| LNE   | March 2022                 | Agilent 7890 GC-FID  | Agilent HP-Plot-U (30 m, 0.53 mm, 20 µm)                     | Dynamic dilution (ISO 6145-7:2018) |
| METAS | January 2022               | Perkin Elmer Clarus 500 GC-FID; thermal desorber TurboMatrix 350   | Agilent DuraBond DB-624 (30 m, 0.32 mm, 1.8 µm)              | Permeation (ISO 6145-10:2002)      |
| VSL   | September 2021, April 2022 | Thermo Trace GC-FID; Markes International thermal desorber Unity 2 | Agilent PoraBond U (25 m, 0.32 mm, 7 µm)                     | Diffusion (ISO 6145-8:2005)        |



805

**Figure B1: Interlaboratory comparison results for methanol. Reported values were the average of 5 measurements, except for month 1 results, which were the average of 3 measurements. Error bars show the expanded uncertainty of the measurements (coverage factor  $k = 2$ ). The dashed line indicates the gravimetric amount fraction of the compound.**

### 810 B.3 RGM stability evaluation

Results of the long-term stability evaluation for two of the prepared RGMs (VSL221418 and VSL221419) are shown in Table B4. The evaluation was carried out immediately after preparation (0–1 month). Other stability periods considered were 5–6 months, 7–8 months, 13–14 months and 18–19 months after preparation of the RGMs.

**Table B4: Temporal stability of two of the gravimetric RGMs. Results are expressed as relative difference ( $\Delta$ ) of the average analytical value with respect to the gravimetric value. Deviations larger than  $\pm 5\%$  are in bold. The stability period is indicated as the number of months after RGM preparation. NA indicates not available data due to an analytical issue during a measurement.**

| RGMs      | Stability period (months) | $\Delta_{\text{acetaldehyde}}$ (%) | $\Delta_{\text{acetone}}$ (%) | $\Delta_{\text{ethanol}}$ (%) | $\Delta_{\text{methacrolein}}$ (%) | $\Delta_{\text{methanol}}$ (%) | $\Delta_{\text{MEK}}$ (%) | $\Delta_{\text{MVK}}$ (%) | $\Delta_{\text{n-hexane}}$ (%) |
|-----------|---------------------------|------------------------------------|-------------------------------|-------------------------------|------------------------------------|--------------------------------|---------------------------|---------------------------|--------------------------------|
| VSL221418 | 0–1                       | -2.2                               | 0.9                           | -1.8                          | -1.3                               | 1.8                            | 3.3                       | -2.7                      | 0.8                            |
|           | 5–6                       | NA                                 | NA                            | NA                            | NA                                 | NA                             | NA                        | NA                        | NA                             |
|           | 7–8                       | <b>9.6</b>                         | 1.2                           | -3.5                          | 0.7                                | <b>-7.1</b>                    | 4.9                       | -3.6                      | 0.9                            |
|           | 13–14                     | <b>16.1</b>                        | 1.9                           | -2.6                          | 3.7                                | <b>-8.4</b>                    | 0.1                       | <b>-6.4</b>               | 1.8                            |
|           | 18–19                     | <b>5.8</b>                         | 0.2                           | -1.4                          | 3.4                                | -4.5                           | -0.1                      | -0.6                      | 0.5                            |
| VSL221419 | 0–1                       | -0.6                               | 0.6                           | -2.0                          | -1.4                               | 0.2                            | 3.1                       | -3.3                      | 0.3                            |
|           | 5–6                       | <b>-7.1</b>                        | 0.4                           | -2.5                          | 0.9                                | <b>7.6</b>                     | <b>5.7</b>                | -4.4                      | -0.6                           |
|           | 7–8                       | <b>8.3</b>                         | 0.9                           | -0.2                          | 0.7                                | <b>7.1</b>                     | 4.6                       | -4.4                      | 0.3                            |
|           | 13–14                     | <b>14.7</b>                        | 1.5                           | 0.1                           | 3.2                                | <b>5.9</b>                     | -0.1                      | <b>-6.2</b>               | 1.2                            |
|           | 18–19                     | <b>5.7</b>                         | -4.7                          | <b>-5.1</b>                   | 3.7                                | -2.5                           | 0.2                       | -0.7                      | -4.7                           |

### Appendix C: Whole air sample spiking and certification

To spike the two parent cylinders with the selected oxygenated volatile organic compounds (OVOCs), a certified Reference Gas Mixture (RGM) filled into a high-pressure 5 L aluminium cylinder (D249650, VSL, Netherlands) was used. The RGM contained acetaldehyde, acetone, ethanol, methacrolein, methanol, methyl ethyl ketone (MEK), methyl vinyl ketone (MVK), benzene, n-hexane and propane in dry nitrogen at amount fractions between 500 and 1004 nmol mol<sup>-1</sup> (Table C1). The cylinder content was transferred to the parent cylinders through a cross connector joined to the outlet of the RGM cylinder (that was heated to avoid condensation), to the parent cylinders and to the vacuum pump used to evacuate the RGM cylinder. Because dilution factors of around 0.011 were expected after whole air filling of the parent cylinders, the RGM cylinder was fully evacuated into the parent cylinders to reach OVOC spiked values between 5 nmol mol<sup>-1</sup> and 10 nmol mol<sup>-1</sup> (Table C1).

**Table C1: Amount fraction ( $x_{\text{cyl}}$ ) and certified expanded uncertainty ( $U(x_{\text{cyl}})$ ) of the OVOCs contained in the gas cylinder used for spiking the air samples. Estimated spiked amount fractions ( $x_{\text{spiked}}$ ) and uncertainties ( $U(x_{\text{spiked}})$ ) in the parent cylinders are also included. The coverage factor of the uncertainty is two ( $k = 2$ ).**

| Compound     | $x_{\text{cyl}}$<br>(nmol mol <sup>-1</sup> ) | $U(x_{\text{cyl}})$<br>(nmol mol <sup>-1</sup> ) | Dilution<br>factor (ratio) | $x_{\text{spiked}}$<br>(nmol mol <sup>-1</sup> ) | $U(x_{\text{spiked}})$<br>(nmol mol <sup>-1</sup> ) |
|--------------|---|--|----------------------------|--|---|
| acetaldehyde | 1000  | 40   | 0.011                      | 10.61  | 0.60  |
| acetone      | 1001  | 30   | 0.011                      | 10.62  | 0.54  |

| Compound     | $x_{cyl}$<br>(nmol mol <sup>-1</sup> ) | $U(x_{cyl})$<br>(nmol mol <sup>-1</sup> ) | Dilution<br>factor (ratio) | $x_{spiked}$<br>(nmol mol <sup>-1</sup> ) | $U(x_{spiked})$<br>(nmol mol <sup>-1</sup> ) |
|--------------|--|---|----------------------------|---|--|
| ethanol      | 866                                    | 43  | 0.011                      | 9.19                                      | 0.59   |
| methacrolein | 991                                    | 30  | 0.011                      | 10.52                                     | 0.53   |
| methanol     | 721                                    | 36  | 0.011                      | 7.65                                      | 0.49   |
| MEK          | 999                                    | 100                                       | 0.011                      | 10.60                                     | 1.15   |
| MVK          | 1002                                   | 50  | 0.011                      | 10.63                                     | 0.68   |
| benzene      | 1004                                   | 30  | 0.011                      | 10.66                                     | 0.54   |
| n-hexane     | 500                                    | 15  | 0.011                      | 5.31                                      | 0.27   |
| propane      | 997                                    | 30  | 0.011                      | 10.58                                     | 0.53   |

835 To produce the SI-traceable working standards of certified spiked whole air samples, six cylinders and 24 canisters (Table C2) were filled with the spiked whole air contained in the two parent cylinders. For that purpose, the parent cylinders were decanted into the selected cylinders and canisters to produce several identical subsamples (i.e., working standards). Four cylinders were 10 L aluminium cylinders with Experis® treatment for non-methane hydrocarbon (NMHC) VOC (Air Products Inc., PA, USA) and two were 3.6 L coated (SilcoNert® 2000) stainless steel cylinders (Swagelok Co., OH, USA). Twelve of the selected canisters were coated with Silonite™ (ten 6 L stainless steel canisters and two 15 L stainless steel canisters; Entech Instruments, CA, USA) and twelve were coated with Silcosteel® (6 L stainless steel; Restek Corporation, PA, USA).

840

**Table C2: Air sample cylinders (\_cyl) and canisters (\_can) used to perform one of the described actions: certification (C), assessment (A) and stability (S).**

| Vessel<br>MVOC151- | Tank S/N   | Tank wall<br>material        | Coating/<br>Treatment | Tank<br>volume<br>(L) | Tank final<br>pressure<br>(·10 <sup>3</sup> hPa) | Action | Participant   |
|--------------------|------------|------------------------------|-----------------------|-----------------------|--|--------|---|
| 001A_cyl           | APE201891  | Aluminium <sup>1</sup>       | Experis®              | 10                    | 105  | C      | VSL <sup>a</sup>  |
| 001B_cyl           | APE917209  | Aluminium <sup>1</sup>       | Experis®              | 10                    | 105  | A      | Empa <sup>b</sup> , DWD <sup>c</sup> , IMT <sup>d</sup> , UU <sup>e</sup>         |
| 001C_cyl           | APE1047602 | Aluminium <sup>1</sup>       | Experis®              | 10                    | 105  | C      | METAS <sup>f</sup>  |
| 001D_cyl           | APE152484  | Aluminium <sup>1</sup>       | Experis®              | 10                    | 105  | S      | Empa <sup>b</sup>   |
| 002A_cyl           | UD2034     | Stainless steel <sup>2</sup> | SilcoNert® 2000       | 3.6                   | 98.8   | C      | VSL <sup>a</sup> , METAS <sup>f</sup>   |
| 002B_cyl           | UU9013     | Stainless steel <sup>2</sup> | SilcoNert® 2000       | 3.6                   | 98.8   | S/A    | Empa <sup>b</sup> /Empa <sup>b</sup> , DWD,<br>IMT <sup>d</sup> , UU <sup>e</sup> |
| 003A_can           | 2566       | Stainless steel <sup>3</sup> | Silonite™             | 15                    | 4.08   | C      | VSL <sup>a</sup> , METAS <sup>f</sup>   |
| 003B_can           | 2565       | Stainless steel <sup>3</sup> | Silonite™             | 15                    | 4.08   | S/A    | Empa <sup>b</sup> /Empa <sup>b</sup> , DWD,<br>IMT <sup>d</sup> , UU <sup>e</sup> |
| 004A_can           | 12938      | Stainless steel <sup>3</sup> | Silonite™             | 6                     | 3.50   | C      | METAS <sup>f</sup>  |
| 004B_can           | 5690       | Stainless steel <sup>3</sup> | Silonite™             | 6                     | 3.50   | C      | METAS <sup>f</sup>  |

| Vessel<br>MVOC151- | Tank S/N | Tank wall<br>material        | Coating/<br>Treatment | Tank<br>volume<br>(L) | Tank final<br>pressure<br>( $\cdot 10^3$ hPa) | Action | Participant        |
|--------------------|----------|------------------------------|-----------------------|-----------------------|---|--------|--------------------|
| 004C_can           | 12200    | Stainless steel <sup>3</sup> | Silonite™             | 6                     | 3.50  | A      | IMT <sup>d</sup>   |
| 004D_can           | 11330    | Stainless steel <sup>3</sup> | Silonite™             | 6                     | 3.50  | A      | UU <sup>e</sup>    |
| 004E_can           | 12202    | Stainless steel <sup>3</sup> | Silonite™             | 6                     | 3.50  | S/A    | Empa <sup>b</sup>  |
| 005A_can           | 5358     | Stainless steel <sup>3</sup> | Silonite™             | 6                     | 3.50  | S/A    | Empa <sup>b</sup>  |
| 005B_can           | 3590     | Stainless steel <sup>3</sup> | Silonite™             | 6                     | 3.50  | C      | VSL <sup>a</sup>   |
| 005C_can           | 5685     | Stainless steel <sup>3</sup> | Silonite™             | 6                     | 3.50  | C      | VSL <sup>a</sup>   |
| 005D_can           | 12204    | Stainless steel <sup>3</sup> | Silonite™             | 6                     | 3.50  | A      | DWD <sup>c</sup>   |
| 005E_can           | 12201    | Stainless steel <sup>3</sup> | Silonite™             | 6                     | 3.50  | C      | METAS <sup>f</sup> |
| 006A_can           | 5032     | Stainless steel <sup>4</sup> | Siltek®               | 6                     | 4.09  | S/A    | Empa <sup>b</sup>  |
| 006B_can           | 5040     | Stainless steel <sup>4</sup> | Siltek®               | 6                     | 4.09  | C      | METAS <sup>f</sup> |
| 006C_can           | 5043     | Stainless steel <sup>4</sup> | Siltek®               | 6                     | 4.09  | A      | IMT <sup>d</sup>   |
| 006D_can           | 5033     | Stainless steel <sup>4</sup> | Siltek®               | 6                     | 4.09  | C      | VSL <sup>a</sup>   |
| 007A_can           | 5041     | Stainless steel <sup>4</sup> | Siltek®               | 6                     | 4.16  | C      | METAS <sup>f</sup> |
| 007B_can           | 5036     | Stainless steel <sup>4</sup> | Siltek®               | 6                     | 4.16  | C      | VSL <sup>a</sup>   |
| 007C_can           | 5045     | Stainless steel <sup>4</sup> | Siltek®               | 6                     | 4.16  | A      | UU <sup>e</sup>    |
| 007D_can           | 5038     | Stainless steel <sup>4</sup> | Siltek®               | 6                     | 4.16  | S/A    | Empa <sup>b</sup>  |
| 008A_can           | 5037     | Stainless steel <sup>4</sup> | Siltek®               | 6                     | 4.08  | C      | METAS <sup>f</sup> |
| 008B_can           | 5039     | Stainless steel <sup>4</sup> | Siltek®               | 6                     | 4.08  | A      | DWD <sup>c</sup>   |
| 008C_can           | 5030     | Stainless steel <sup>4</sup> | Siltek®               | 6                     | 4.08  | S/A    | Empa <sup>b</sup>  |
| 008D_can           | 5034     | Stainless steel <sup>4</sup> | Siltek®               | 6                     | 4.08  | C      | VSL <sup>a</sup>   |

<sup>1</sup>Air Products, <sup>2</sup>Swagelok, <sup>3</sup>ENTECH Instruments, <sup>4</sup>RESTEK

<sup>a</sup>National Metrology Institute (NMI) of the Netherlands, <sup>b</sup>Swiss Federal Laboratories for Materials Science and Technology, <sup>c</sup>Deutscher Wetterdienst, <sup>d</sup>Institute Mines-Télécom, <sup>e</sup>Utrecht University and <sup>f</sup>NMI of Switzerland

845

**Table C3: Results of the homogeneity test performed on a subset of vessels filled with the SI-traceable working standards based on certified spiked whole air samples. The amount fractions ( $x_a$ ) and standard deviations (SD) correspond to three replicates analysed by Empa for each vessel, including the parent cylinders (E-202A, E-202B).**

| vessel       | acetaldehyde<br>(nmol mol <sup>-1</sup> ) |      | acetone<br>(nmol mol <sup>-1</sup> ) |      | ethanol<br>(nmol mol <sup>-1</sup> ) |      | MEK<br>(nmol mol <sup>-1</sup> ) |      | methanol<br>(nmol mol <sup>-1</sup> ) |      | MVK<br>(nmol mol <sup>-1</sup> ) |      |
|--------------|---|------|--------------------------------------|------|--------------------------------------|------|----------------------------------|------|---------------------------------------|------|----------------------------------|------|
|              | $x_a$                                     | SD   | $x_a$                                | SD   | $x_a$                                | SD   | $x_a$                            | SD   | $x_a$                                 | SD   | $x_a$                            | SD   |
| MVOC151-001D | 18.91                                     | 0.02 | 16.74                                | 0.15 | 7.52                                 | 0.10 | 10.32                            | 0.05 | 6.19                                  | 0.15 | 5.62                             | 0.03 |
| MVOC151-002B | 20.66                                     | 0.08 | 16.56                                | 0.18 | 7.14                                 | 0.08 | 10.20                            | 0.21 | 6.97                                  | 0.11 | 6.29                             | 0.08 |
| MVOC151-003B | 19.67                                     | 0.13 | 19.70                                | 0.22 | 9.34                                 | 0.10 | 11.03                            | 0.14 | 20.69*                                | 0.27 | 6.46                             | 0.06 |
| MVOC151-004E | 18.82                                     | 0.36 | 17.15                                | 0.07 | 8.61                                 | 0.08 | 11.09                            | 0.07 | 9.08                                  | 0.66 | 6.51                             | 0.06 |
| MVOC151-006A | 21.09                                     | 0.50 | 17.28                                | 0.06 | 7.99                                 | 0.10 | 11.48                            | 0.22 | 9.42                                  | 0.18 | 6.84                             | 0.09 |
| MVOC151-007D | 19.74                                     | 0.45 | 17.61                                | 0.06 | 8.66                                 | 0.21 | 12.17                            | 0.14 | 10.19                                 | 0.07 | 7.13                             | 0.05 |

| vessel       | acetaldehyde<br>(nmol mol <sup>-1</sup> ) |      | acetone<br>(nmol mol <sup>-1</sup> ) |      | ethanol<br>(nmol mol <sup>-1</sup> ) |      | MEK<br>(nmol mol <sup>-1</sup> ) |      | methanol<br>(nmol mol <sup>-1</sup> ) |      | MVK<br>(nmol mol <sup>-1</sup> ) |      |
|--------------|---|------|--------------------------------------|------|--------------------------------------|------|----------------------------------|------|---------------------------------------|------|----------------------------------|------|
|              | $x_a$                                     | SD   | $x_a$                                | SD   | $x_a$                                | SD   | $x_a$                            | SD   | $x_a$                                 | SD   | $x_a$                            | SD   |
| MVOC151-008C | 19.76                                     | 0.32 | 17.27                                | 0.08 | 8.96                                 | 0.08 | 11.78                            | 0.09 | 10.22                                 | 0.10 | 7.00                             | 0.03 |
| E-202A       | 17.48                                     | 0.10 | 16.36                                | 0.11 | 7.52                                 | 0.16 | 10.18                            | 0.12 | 7.32                                  | 0.07 | 6.86                             | 0.07 |
| E-202B       | 17.53                                     | 0.09 | 17.58                                | 0.06 | 7.44                                 | 0.14 | 10.62                            | 0.07 | 5.61                                  | 0.10 | 6.82                             | 0.06 |

850 \*outlier

Certification of the air samples was done using two Thermal Desorption-Gas Chromatography-Flame Ionization Detector (TD-GC-FID) systems (Table C4) and following the same measurement sequence: blanks, air sample, calibration standard at low amount fraction level (1–24 nmol mol<sup>-1</sup>, depending on the compound), air sample and calibration standard at high amount fraction level (10–45 nmol mol<sup>-1</sup>, depending on the compound). VSL calibration standards consisted of two multi-compound gas mixtures at 2 nmol mol<sup>-1</sup> and 10 nmol mol<sup>-1</sup> for acetone, methanol, ethanol, acetaldehyde, methacrolein, methyl vinyl ketone (MVK) and methyl ethyl ketone (MEK) in nitrogen. The calibration standards were prepared by diluting two gravimetric RGMs containing these OVOCs in nitrogen, as well as n-hexane and propane, at 100 nmol mol<sup>-1</sup> and 1000 nmol mol<sup>-1</sup>. An additional calibration standard containing acetone, ethanol, methanol and n-hexane in clean and dry air at ca. 10 nmol mol<sup>-1</sup> was obtained by diffusion. METAS generated calibration standards containing acetaldehyde, acetone, ethanol, methacrolein, methanol and MVK in nitrogen at around 10 nmol mol<sup>-1</sup> by the permeation method (ISO 6145-10:2002 (ISO, 2002)) using a magnetic suspension balance (Waters, DE, USA) and a portable generator (Pascale et al., 2017).

**Table C4: Analytical methods used for the certification of air samples**

| Lab   | Date      | Analytical instrument  | Capillary column<br>(length, internal diameter,<br>film thickness)                                 | Sampling method  |
|-------|-----------|--|--|--|
| VSL   | Jul. 2021 | Thermo Trace GC-FID;<br>Markes International<br>thermal desorber Unity 2 | Agilent PoraBond U<br>(25 m, 0.32 mm, 7 µm)<br>Restek Stabilwax for MVK<br>(30 m, 0.32 mm, 1.0 µm) | Autosampler (600 mL sampling volume)   |
| METAS | Feb. 2022 | Perkin Elmer Clarus 500<br>GC-FID; thermal desorber<br>TurboMatrix 350   | Agilent DuraBond DB-624<br>(30 m, 0.32 mm, 1.8 µm)   | Carbograph 2 (60/80) – Carbograph 1<br>(40/60) – Carbosieve™ SIII (60/80)<br>multibed sorbent tubes (300–750 mL<br>loading volume) |

865 The uncertainty of the assigned amount fraction of each compound and air sample was the result of multiplying the combined uncertainty of each air sample by the coverage factor ( $k = 2$ ). The combined uncertainty was estimated as the combination of the uncertainty of the calibration standards, the mean standard deviation of the measurements results and the pooled standard deviation of the measurements (Eq. (C1)).

$$870 \quad u^2(x_{sample}) = x_{sample}^2 \left( \frac{u^2(x_{cal})}{x_{cal}^2} + \frac{u^2(\overline{RF}_{cal})}{\overline{RF}_{cal}^2} + \frac{u^2(\overline{y}_{sample})}{\overline{y}_{sample}^2} + u^2(pooled\_sd) \right) \quad (C1)$$

where,

$u(x_{sample})$ : uncertainty of the assigned amount fraction of the compound in the air sample

$x_{sample}$ : assigned amount fraction of the compound in the air sample

$u(x_{cal})$ : uncertainty of the amount fraction of the compound in the calibration standard

875  $x_{cal}$ : amount fraction of the compound in the calibration standard

$u(\overline{RF}_{cal})$ : mean standard deviation of the response factor of the compound calibration standard

$\overline{RF}_{cal}$ : average response factor of the compound calibration standard (average of three measurements)

$u(\overline{y}_{sample})$ : mean standard deviation of the GC-FID compound responses (average of three measurements)

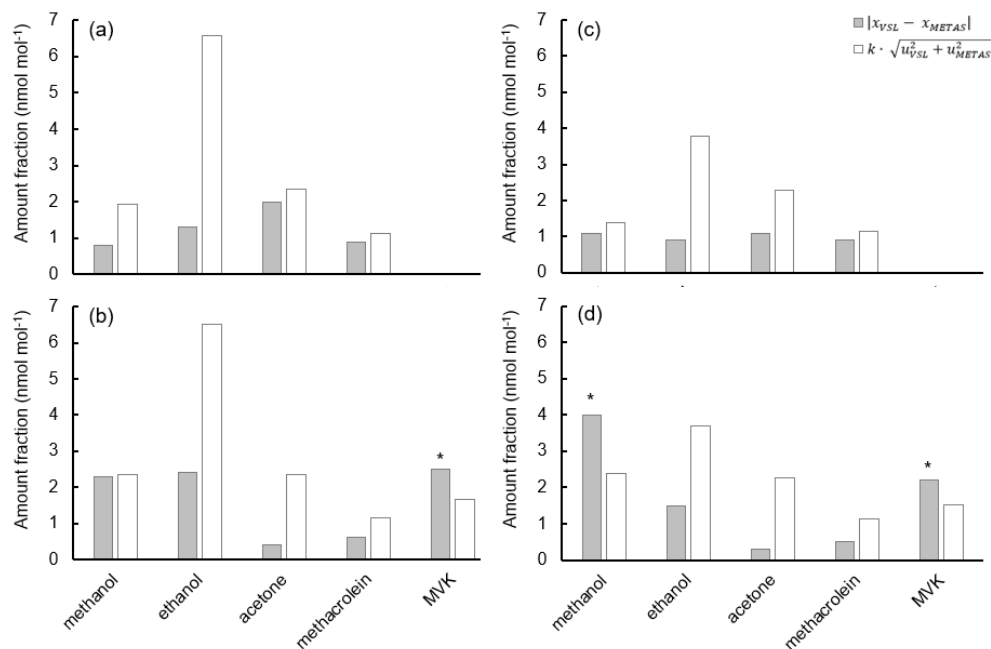
$\overline{y}_{sample}$ : average GC-FID compound response (average of three measurements)

880  $u(pooled\_sd)$ : pooled standard deviation of the measurement results

**Table C5: Analytical amount fraction values ( $x_a$ ) and their expanded uncertainty ( $U$ ; coverage factor  $k = 2$ ) obtained by the two National Metrology Institutes (NMIs) certifying the air samples: VSL and METAS.**

| vessel   | NMI   | date    | methanol<br>(nmol mol <sup>-1</sup> ) |          | ethanol<br>(nmol mol <sup>-1</sup> ) |          | acetone<br>(nmol mol <sup>-1</sup> ) |          | methacrolein<br>(nmol mol <sup>-1</sup> ) |          |
|----------|-------|---------|---------------------------------------|----------|--------------------------------------|----------|--------------------------------------|----------|---|----------|
|          |       |         | $x_a$                                 | $U(x_a)$ | $x_a$                                | $U(x_a)$ | $x_a$                                | $U(x_a)$ | $x_a$                                     | $U(x_a)$ |
| MVOC151- |       |         |                                       |          |                                      |          |                                      |          |   |          |
| 001A     | VSL   | 07/2021 | 11.5                                  | 0.7      | 11.1                                 | 1.0      | 18.2                                 | 1.9      | 11.5                                      | 0.7      |
| 001A     | VSL   | 09/2022 | 14.6                                  | 1.5      | 10.0                                 | 0.5      | 16.6                                 | 0.6      | 10.0                                      | 0.6      |
| 001C     | METAS | 02/2022 | 12.3                                  | 1.8      | 12.4                                 | 6.5      | 16.2                                 | 1.4      | 10.6                                      | 0.9      |
| 002A     | VSL   | 07/2021 | 9.2*                                  | 0.5      | 8.7                                  | 0.8      | 17.9                                 | 1.8      | 11.0                                      | 0.7      |
| 002A     | METAS | 02/2022 | 8.1*                                  | 1.3      | 7.8                                  | 3.7      | 16.8                                 | 1.4      | 10.1                                      | 0.9      |
| 002A     | VSL   | 09/2022 | 12.1*                                 | 2.0      | 6.3                                  | 0.3      | 17.1                                 | 1.2      | 9.6                                       | 0.6      |
| 003A     | VSL   | 07/2021 | 21.9*                                 | 1.8      | 11.8*                                | 1.1      | 18.9*                                | 1.9      | 18.1*                                     | 1.0      |
| 003A     | METAS | 02/2022 | 15.2*                                 | 1.4      | 6.0*                                 | 2.7      | 15.4*                                | 1.5      | 9.9*                                      | 0.9      |
| 005B     | VSL   | 07/2021 | 8.2                                   | 0.8      | 10.1*                                | 0.9      | 14.1*                                | 1.4      | 8.5                                       | 0.5      |
| 005E     | METAS | 02/2022 | 8.9                                   | 1.5      | 1.4*                                 | 0.8      | 11.4*                                | 1.6      | 8.9                                       | 1.3      |
| 007B     | VSL   | 07/2021 | 4.2*                                  | 0.8      | 10.2*                                | 0.9      | 14.3                                 | 1.4      | 8.7                                       | 0.5      |
| 007A     | METAS | 02/2022 | 7.5*                                  | 0.9      | 2.0*                                 | 1.1      | 12.5                                 | 1.6      | 9.3                                       | 0.9      |

\*values for which the criterion described in Eq. (4) was not fulfilled



890 **Figure C1:** Representation of the consistency of the amount fraction values assigned to the 10 L Experis cylinders according to the criterion described in Eq. (4). METAS measurements (vessel 001C and 002A) performed in February 2022 were compared to the VSL measurements carried out in July 2021 on vessel 001A (a) and 002A (c) and in September 2022 on vessel 001A (b) and 002A (d). The asterisks show those measurements for which the absolute difference of the measured amount fractions ( $x_{VSL}$ ,  $x_{METAS}$ ) was greater than twice (coverage factor  $k = 2$ ) the square root of the sum of squares of the measurement standard uncertainties ( $u_{VSL}$ ,  $u_{METAS}$ ).

## Appendix D: Assessment of the working standards traceable to the international system of units (SI)

### D.1 In-house working standards

895 The analytical instruments selected to assess the SI-traceable working standards (Appendix A; Table A1) were calibrated with in-house working standards generated using different methods.

The Thermal Desorption-Gas Chromatography-Flame Ionization Detector/Mass Spectrometry (TD-GC-FID/MS) system used by DWD (Deutscher Wetterdienst) to assess the working standards based on certified spiked whole air samples was calibrated using one of the Reference Gas Mixtures (RGMs) prepared by the national metrology institute (NMI) of the Netherlands (VSL) for this work (oxygenated volatile organic compounds (OVOCs) in nitrogen at 100 nmol mol<sup>-1</sup>) without further dilution. In addition, DWD TD-GC-FID/MS system was calibrated using a primary reference material containing 30 non-methane hydrocarbons (NMHCs) considered ozone precursors at amount fraction levels of 2 nmol mol<sup>-1</sup> (NPL NMHC standard; Grenfell et al., 2010). The same type of standard (NPL NMHC) was used to calibrate Empa TD-GC-FID.

905 The ion transmission curves of both Proton Transfer Reaction-Time of Flight-Mass Spectrometry (PTR-ToF-MS) were determined using a SI-traceable certified reference material produced by the National Physical Laboratory (NPL), the NMI of the United Kingdom (Worton et al., 2023) as in-house working standards (NPL PTR-MS standard). The in-house working

standards (NPL D961410 used by Institute Mines-Télécom (IMT) and D961397 used by Utrecht University (UU)) contained 20 compounds at amount fractions around  $1 \mu\text{mol mol}^{-1}$  covering a mass spectrum from  $m/z$  33 to  $m/z$  671. Prior to instrument calibration, the in-house working standards were diluted with zero air (i.e. dry nitrogen) down to amount fractions  $< 10 \text{ nmol mol}^{-1}$ .

VSL TD-GC-FID was calibrated using RGMs based on the diffusion method (dynamic preparation method ISO 6145-8) as in-house working standards for acetone, ethanol, methacrolein, methanol, methyl ethyl ketone (MEK) and methyl vinyl ketone (MVK). For acetaldehyde, an in-house working standard was obtained by dynamic dilution of a  $1 \mu\text{mol mol}^{-1}$  multi-component RGM containing acetaldehyde, acetone, ethanol, methacrolein, methanol, MEK, MVK and propane in nitrogen. Three to six in-house working standards were prepared in the range  $4\text{--}20 \text{ nmol mol}^{-1}$ .

## D.2 Measurement procedure for assessing the working standards based on dynamic dilution of RGMs

Samples were prepared by dynamic dilution of RGMs. VSL, IMT and UU generated two samples. VSL set the same dilution factor for both samples (10 times dilution to obtain OVC amount fractions close to  $10 \text{ nmol mol}^{-1}$ ), while the Swiss Federal Laboratories for Materials Science and Technology (Empa) and IMT used different dilution factors (Table D1). UU prepared six samples using different dilution factors (Table D1).

Before performing the measurement sequence, VSL sampled and analysed 15 times the pure nitrogen used for dilution to clean the analytical system and to assess the system blank. Each in-house standard (three to six in total) and sample (i.e., SI-traceable working standard) was sampled at a flow rate of  $20 \text{ mL min}^{-1}$  for 30 minutes.

Empa ran five to ten GC runs with a sample of similar humidity level and composition that the matrix gas to condition the GC-FID. After the conditioning, six consecutive runs without injecting any sample were measured to estimate the system blank. Then, six in-house working standard runs were followed by six runs for each sample (i.e., SI-traceable working standard). In-house working standard and blank runs (12 runs in total) were repeated after the last sample measurement. Sampling volume was set at 300 mL ( $20 \text{ minutes at } 15 \text{ mL min}^{-1}$ ).

IMT measurement sequence started with 30 minutes of zero air sampling to quantify background signals and to verify signal stability. The zero air was obtained using a catalytic converter containing platinum wool (high sensitivity catalyst for TOC analyser, Shimadzu Corporation, Japan), which was heated up to  $350 \text{ }^\circ\text{C}$ . Blank measurements were performed before and after each new sample test and calibration. After the first blank measurements, the calibration took place by analysing in-house working standards during 60–90 minutes. The in-house working standards ( $5 \text{ mL min}^{-1}$ ) were diluted with a zero-air flow rate of  $1 \text{ L min}^{-1}$ . Flows were regulated by MFCs in a Gas Calibration Unit (GCU, Ionico Analytik GmbH, Austria). Then, each sample was analysed for 90 minutes. The same sampling line coated with SilcoNert® 1000 and sampling flow rate of  $100 \text{ mL min}^{-1}$  were used for blanks, calibration standards and samples.

UU measured each sample 2–4 times for at least 30 seconds. Before and after each sample measurement, UU analysed blanks (i.e., zero air produced by a heated platinum catalyst) and the in-house working standard (NPL-PTR-MS standard). Blanks,



940 in-house working standards and samples were injected through a sample loop (250  $\mu\text{L}$  volume) according the procedure described in Holzinger et al. (2019). The in-house working standards (loop flow of 10  $\text{mL min}^{-1}$ ) were diluted with a zero-air flow of 240  $\text{mL min}^{-1}$ . Sample flows, depending on the pressure in cylinders and canisters, were produced between 80  $\text{mL min}^{-1}$  and 300  $\text{mL min}^{-1}$ .

### 945 D.3 Measurement procedure for assessing working standards based on certified whole air samples

The same air sample cylinders were assessed by the participants (round-robin comparison). However, different canisters were sent to the participants because of the low sample volume, which was enough only for one analysis (Table C2). Participants followed a similar measurement sequence than the measurement procedure described for the SI-traceable working standards based on RGM dilution. After some blank measurements (six times for GC-FID and 30 minutes for PTR-ToF-MS), in-house  
 950 working standards were measured at minimum two amount fraction levels (six times per level for GC-FID and for PTR-ToF-MS, IMT measured for 90 min and UU for 1 min). Samples were measured between calibration levels (6 times each sample for GC-FID and 90 minutes per sample for PTR-ToF-MS measurements at IMT and 1 min at UU). Blank measurements were performed again after the second amount fraction level of the calibration.

955 **Table D1: Flow rates (in  $\text{mL min}^{-1}$ ) and relative expanded uncertainty (coverage factor  $k = 2$ ) of the dilution systems used to dilute VSL SI-traceable RGM during the assessment of SI-traceable working standards by each laboratory. Gas flow rates correspond to the flow rate of VSL SI-traceable RGM ( $q_{v\_RGM}$ ), first-step dilution flow rate ( $q_{v\_d1}$ ), split flow rate ( $q_{v\_sp}$ ) and second-step dilution flow ( $q_{v\_d2}$ ). The assigned amount fractions of the selected compounds are shown together with their expanded uncertainties ( $k = 2$ ), both expressed in  $\text{nmol mol}^{-1}$ .**

|       | $q_{v\_RGM}$<br>$\pm U$ (%) | $q_{v\_d1}$<br>$\pm U$ (%) | $q_{v\_sp}$<br>$\pm U$ (%) | $q_{v\_d2}$<br>( $\pm 0.3\%$ ) | $x_{acetaldehyde}$<br>$\pm U$ | $x_{acetone}$<br>$\pm U$ | $x_{methanol}$<br>$\pm U$ | $x_{MEK}$<br>$\pm U$ | $x_{MVK}$<br>$\pm U$ |
|-------|-----------------------------|----------------------------|----------------------------|--------------------------------|-------------------------------|--------------------------|---------------------------|----------------------|----------------------|
| VSL1  | 109 $\pm$ 0.5               | 917 $\pm$ 0.5              | -                          | -                              | NA                            | 10.58 $\pm$ 0.38         | 10.57 $\pm$ 0.64          | 10.56 $\pm$ 0.34     | 10.74 $\pm$ 0.38     |
| VSL2  | 109 $\pm$ 0.5               | 913 $\pm$ 0.5              | -                          | -                              | 10.87 $\pm$ 0.99              | 10.59 $\pm$ 0.38         | 10.58 $\pm$ 0.64          | 10.57 $\pm$ 0.34     | 10.74 $\pm$ 0.38     |
| IMT1  | 100 $\pm$ 0.4               | 520 $\pm$ 0.3              | -                          | -                              | 16.4 $\pm$ 1.5                | 16.12 $\pm$ 0.59         | 16.96 $\pm$ 0.81          | 15.87 $\pm$ 0.56     | 16.13 $\pm$ 0.94     |
| IMT2  | 60 $\pm$ 0.4                | 520 $\pm$ 0.3              | -                          | -                              | 10.56 $\pm$ 0.99              | 10.34 $\pm$ 0.38         | 10.88 $\pm$ 0.52          | 10.18 $\pm$ 0.35     | 10.34 $\pm$ 0.61     |
| UU1   | 45 $\pm$ 0.4                | 1455 $\pm$ 0.3             | 100 $\pm$ 0.5              | 1400 $\pm$ 0.3                 | 0.30 $\pm$ 0.09               | 0.21 $\pm$ 0.02          | 0.22 $\pm$ 0.02           | 0.20 $\pm$ 0.01      | 0.20 $\pm$ 0.02      |
| UU2   | 90 $\pm$ 0.4                | 1400 $\pm$ 0.3             | 100 $\pm$ 0.5              | 1410 $\pm$ 0.3                 | 0.49 $\pm$ 0.09               | 0.40 $\pm$ 0.02          | 0.42 $\pm$ 0.03           | 0.38 $\pm$ 0.02      | 0.39 $\pm$ 0.03      |
| UU3   | 12 $\pm$ 0.4                | 1488 $\pm$ 0.3             | -                          | -                              | 0.91 $\pm$ 0.11               | 0.81 $\pm$ 0.04          | 0.85 $\pm$ 0.05           | 0.79 $\pm$ 0.03      | 0.80 $\pm$ 0.05      |
| UU4   | 24 $\pm$ 0.4                | 1476 $\pm$ 0.3             | -                          | -                              | 1.72 $\pm$ 0.18               | 1.61 $\pm$ 0.06          | 1.69 $\pm$ 0.09           | 1.58 $\pm$ 0.06      | 1.60 $\pm$ 0.10      |
| UU5   | 30 $\pm$ 0.4                | 1470 $\pm$ 0.3             | -                          | -                              | 2.12 $\pm$ 0.21               | 2.01 $\pm$ 0.08          | 2.11 $\pm$ 0.11           | 1.97 $\pm$ 0.07      | 2.00 $\pm$ 0.12      |
| UU6   | 60 $\pm$ 0.4                | 1440 $\pm$ 0.3             | -                          | -                              | 4.14 $\pm$ 0.39               | 4.00 $\pm$ 0.16          | 4.21 $\pm$ 0.21           | 3.94 $\pm$ 0.14      | 4.00 $\pm$ 0.24      |
| Empa1 | 14 $\pm$ 0.4                | 650 $\pm$ 0.3              | -                          | -                              | 2.34 $\pm$ 0.23               | 2.14 $\pm$ 0.10          | 2.18 $\pm$ 0.15           | 2.18 $\pm$ 0.09      | 2.22 $\pm$ 0.08      |
| Empa2 | 20 $\pm$ 0.4                | 1450 $\pm$ 0.3             | -                          | -                              | 1.51 $\pm$ 0.15               | 1.35 $\pm$ 0.07          | 1.37 $\pm$ 0.10           | 1.37 $\pm$ 0.06      | 1.40 $\pm$ 0.06      |

#### 960 D.4 IMT measured amount fractions

IMT estimated the amount fractions of the selected OVOCs according to the calibration approach described in de Gouw and Warneke (2007) and following Eq. (D1). In practice, a sensitivity factor of  $\text{H}_3\text{O}^+$  normalized to  $10^6$  cps ( $S_N(\text{RH}^+)$ ) is derived for each targeted compound during calibration experiments. This sensitivity factor comprises the parameters:  $k_{PTR}$ ,  $\Delta t$ ,  $T(\text{RH}^+)$  and  $T(\text{H}_3\text{O}^+)$ . The approach used in de Gouw and Warneke (2007) to account for humidity-dependent sensitivities was applied in this work.

$$x_i = \frac{1}{k_{PTR} \Delta t} \cdot \frac{I(\text{RH}^+)}{T(\text{RH}^+)} \cdot \left( \frac{I(\text{H}_3\text{O}^+)}{T(\text{H}_3\text{O}^+)} \right)^{-1} = \frac{I(\text{RH}^+) \cdot 10^6}{S_N(\text{RH}^+) \cdot I(\text{H}_3\text{O}^+)} \quad (\text{D1})$$

where,

$x_i$ : amount fraction of the compound  $R$  (i.e., OVOC under study)

$k_{PTR}$ : proton-transfer-reaction rate coefficient of  $\text{R} + \text{H}_3\text{O}^+ \rightarrow \text{RH}^+ + \text{H}_2\text{O}$

970  $\Delta t$ : reaction time in the drift tube

$I(\text{RH}^+)$ : observed signal (counts per second, cps) for the protonated ion  $\text{RH}^+$

$I(\text{H}_3\text{O}^+)$ : observed signal (cps) for the reagent ion  $\text{H}_3\text{O}^+$

$T(\text{RH}^+)$ : transmission efficiency for  $\text{RH}^+$

$T(\text{H}_3\text{O}^+)$ : transmission efficiency for  $\text{H}_3\text{O}^+$

975  $S_N(\text{RH}^+)$ : sensitivity factor of  $\text{H}_3\text{O}^+$  normalized to  $10^6$  cps.

Sources of uncertainty associated to the measured amount fractions included the precision of the system and the calibration accuracy. The uncertainty linked to the precision of the system ( $u_{prec}$ ) was calculated according Eq. (D2). The uncertainty associated to the calibration accuracy ( $u_{cal\_acc}$ ) was estimated applying Eq. (D3).

980

$$u_{prec} = \frac{\sqrt{I_m(\text{RH}^+) + I_z(\text{RH}^+)}}{S_N(\text{RH}^+) \cdot I(\text{H}_3\text{O}^+)} \cdot 10^6 \quad (\text{D2})$$

where,

$u_{prec}$ : measurement precision expressed as amount fraction

985  $I_m(\text{RH}^+)$ :  $\text{RH}^+$  signal (cps) observed when a sample was measured

$I_z(\text{RH}^+)$ :  $\text{RH}^+$  signal (cps) observed when zeroing the instrument

$I(\text{H}_3\text{O}^+)$ : observed signal (cps) for the reagent ion  $\text{H}_3\text{O}^+$

$S_N(\text{RH}^+)$ : sensitivity factor of  $\text{H}_3\text{O}^+$  normalized to  $10^6$  cps

$$990 \quad \frac{u_{cal\_acc}}{x_{cal}} = \sqrt{\left(\frac{u(x_{cyl})}{x_{cyl}}\right)^2 + \frac{1}{(q_{v\_cal} + q_{v\_dil})^2} \cdot \left(\frac{q_{v\_dil}^2}{q_{v\_cal}^2} \cdot u(q_{v\_cal})^2 + u(q_{v\_dil})^2\right)} \quad (D3)$$

where,

$u_{cal\_acc}$ : relative combined uncertainty of the calibration accuracy

$x_{cal}$ : OVOC amount fraction generated after dilution of the calibration standard

$u(x_{cyl})$ : standard uncertainty of the OVOC amount fraction in the calibration standard (calibration certificate)

995  $x_{cyl}$ : OVOC amount fraction in the calibration standard (calibration certificate)

$q_{v\_cal}$ : flow rate of the calibration standard

$q_{v\_dil}$ : flow rate of the dilution gas

$u(q_{v\_cal})$ : standard uncertainty of the calibration standard flow rate

$u(q_{v\_dil})$ : standard uncertainty of the dilution gas flow rate

1000

## D.5 Uncertainty of the measurements performed to assess the SI-traceable working standards

Tables D2 and D3 show the amount fraction results of the measurements performed by the participants on the assessment of the SI-traceable working standards for each of the selected OVOCs.

1005 **Table D2: Amount fractions ( $x_i$ ) of the selected OVOCs measured by the participants on the assessment of the SI-traceable working standards based on the dilution of RGMs. Expanded uncertainty ( $U$ , coverage factor  $k = 2$ ) of the measurements are indicated together with the amount fractions, both expressed in  $\text{nmol mol}^{-1}$ .**

| Sample | analytical<br>method | calibration<br>standard | $x_{acetaldehyde}$<br>$\pm U$ | $x_{acetone}$<br>$\pm U$ | $x_{methanol}$<br>$\pm U$ | $x_{MEK}$<br>$\pm U$ | $x_{MVK}$<br>$\pm U$ |
|--------|----------------------|-------------------------|-------------------------------|--------------------------|---------------------------|----------------------|----------------------|
| IMT1   | PTR-ToF-MS           | NPL PTR-MS              | 26.2±3.9                      | 19.3±4.4                 | 17.3±3.9                  | 18.3±4.1             | NA*                  |
| IMT2   | PTR-ToF-MS           | NPL PTR-MS              | 17.0±3.8                      | 12.4±2.8                 | 12.4±2.8                  | 11.9±2.7             | NA*                  |
| UU1    | PTR-ToF-MS           | NPL PTR-MS              | 0.23±0.03                     | 0.22±0.03                | 0.12±0.02                 | 0.17±0.03            | NA*                  |
| UU2    | PTR-ToF-MS           | NPL PTR-MS              | 0.42±0.06                     | 0.40±0.06                | 0.23±0.03                 | 0.35±0.05            | NA*                  |
| UU3    | PTR-ToF-MS           | NPL PTR-MS              | 0.75±0.11                     | 0.70±0.11                | 0.46±0.07                 | 0.58±0.09            | NA*                  |
| UU4    | PTR-ToF-MS           | NPL PTR-MS.             | 1.65±0.25                     | 1.64±0.25                | 1.27±0.19                 | 1.47±0.22            | NA*                  |
| UU5    | PTR-ToF-MS           | NPL PTR-MS              | 1.97±0.3                      | 1.81±0.27                | 0.85±0.13                 | 1.49±0.22            | NA*                  |
| UU6    | PTR-ToF-MS           | NPL PTR-MS              | 4.03±0.6                      | 3.56±0.53                | 1.50±0.23                 | 2.93±0.44            | NA*                  |
| Empa1  | TD-GC-FID            | NPL NMHC                | 2.42±0.73                     | 1.35±0.62                | 2.99±0.91                 | 1.63±0.64            | 1.40±0.43            |
| Empa2  | TD-GC-FID            | NPL NMHC                | 1.45±0.45                     | 1.11±0.38                | 2.03±0.62                 | 0.99±0.39            | 0.83±0.26            |
| VSL1   | TD-GC-FID            | VSL diffusion           | NA                            | 10.79±0.35               | 10.81±0.37                | 10.54±0.34           | 10.55±0.35           |
| VSL2   | TD-GC-FID            | VSL diffusion           | 11.2±1.2                      | 10.88±0.35               | 10.68±0.37                | 10.58±0.34           | 10.38±0.34           |

\* MVK data not available because PTR-ToF-MS can only provide the sum of MVK and methacrolein.

**Table D3: Amount fractions ( $x_i$ ) of the selected OVOCs measured by the participants on the assessment of the SI-traceable working standards based certified spiked whole air samples. Expanded uncertainty ( $U$ , coverage factor  $k = 2$ ) of the measurements are indicated together with the amount fractions, both expressed in  $\text{nmol mol}^{-1}$ . The analytical methods correspond to TD-GC-FID (AM1) and to PTR-ToF-MS (AM2) and the calibration standards to NPL NMHC standard (Std1), METAS permeation standard (Std2), VSL diffusion standard (Std3) and NPL PTR-MS standard (Std4).**

\* MVK data not available because PTR-ToF-MS can only provide the sum of MVK and methacrolein.

| Participant | Vessel   | analytical<br>method | calibration<br>standard | $x_{\text{acetone}}$<br>$\pm U$ | $x_{\text{methanol}}$<br>$\pm U$ | $x_{\text{MEK}}$<br>$\pm U$ | $x_{\text{MVK}}$<br>$\pm U$ |
|-------------|----------|----------------------|-------------------------|---------------------------------|----------------------------------|-----------------------------|-----------------------------|
| DWD         | cyl-001B | AM1                  | Std1                    | 15.98±0.97                      | NA                               | 11.88±0.86                  | 8.43±0.62                   |
| METAS       | cyl-001C | AM1                  | Std2                    | 16.2±1.4                        | 12.3±1.8                         | NA                          | 8.1±1.5                     |
| VSL         | cyl-001A | AM1                  | Std3                    | 16.60±0.60                      | 14.6±1.5                         | 11.20±0.50                  | 10.60±0.60                  |
| Empa        | cyl-001D | AM1                  | Std1                    | 15.99±0.88                      | 13.69±0.84                       | 10.83±0.62                  | 5.32±0.28                   |
| IMT         | cyl-001B | AM2                  | Std4                    | 14.7±3.3                        | 17.7±4.0                         | 10.1±2.3                    | NA*                         |
| UU          | cyl-001B | AM2                  | Std4                    | 16.90±0.68                      | 28.4±4.6                         | 11.00±0.66                  | NA*                         |
| DWD         | cyl-002B | AM1                  | Std1                    | 16.7±1.1                        | NA                               | 11.82±0.86                  | 7.86±0.60                   |
| METAS       | cyl-002A | AM1                  | Std2                    | 16.8±1.4                        | 8.1±1.3                          | NA                          | 7.3±1.4                     |
| VSL         | cyl-002A | AM1                  | Std3                    | 17.1±1.2                        | 12.1±2.0                         | 10.90±0.60                  | 9.5±0.6                     |
| Empa        | cyl-002B | AM1                  | Std1                    | 17.9±1.1                        | 12.22±0.72                       | 12.70±0.74                  | NA*                         |
| IMT         | cyl-002B | AM2                  | Std4                    | 15.6±3.6                        | 8.0±1.9                          | 10.2±2.3                    | NA*                         |
| UU          | cyl-002A | AM2                  | Std4                    | 16.90±0.34                      | 7.4±0.8                          | 9.30±0.37                   | 8.27±0.46                   |
| DWD         | can-005D | AM1                  | Std1                    | 16.96±0.92                      | NA                               | 11.97±0.64                  | 8.02±0.46                   |
| METAS       | can-004A | AM1                  | Std2                    | 13.3±2.6                        | 8.8±1.2                          | NA                          | 6.6±1.4                     |
| VSL         | can-005B | AM1                  | Std3                    | 14.1±1.4                        | 8.2±0.8                          | 10.4±0.9                    | NA                          |
| UU          | can-004D | AM2                  | Std4                    | 16.80±0.34                      | 13.50±0.81                       | 9.50±0.57                   | NA*                         |
| IMT         | can-004C | AM2                  | Std4                    | 17.1±3.9                        | 26.6±6.0                         | 11.4±2.6                    | NA*                         |
| Empa        | can-005A | AM1                  | Std1                    | 18.2±1.4                        | 17.1±2.0                         | 12.9±1.1                    | 8.27±0.62                   |
| DWD         | can-008B | AM1                  | Std1                    | 24.9±1.4                        | NA                               | 15.60±0.84                  | 7.06±0.40                   |
| METAS       | can-007A | AM1                  | Std2                    | 12.5±1.6                        | 8.00±0.90                        | NA                          | 6.7±1.4                     |
| VSL         | can-007B | AM1                  | Std3                    | 14.3±1.4                        | 4.20±0.80                        | 10.30±0.90                  | NA                          |
| UU          | can-007C | AM2                  | Std4                    | 29.9±2.4                        | 22.60±0.90                       | 15.5±1.9                    | NA*                         |
| Empa        | can-007D | AM2                  | Std1                    | 16.47±0.90                      | 14.19±0.88                       | 14.45±0.88                  | 7.53±0.40                   |

**Data availability**

Data used in this work is available on the MetClimVOC Zenodo community: <https://doi.org/10.5281/zenodo.14178374> (Iturrate-Garcia et al., 2024).

**Author contribution**

1020 SR, PS, CP, MI-G, AB, TS, AC and RH designed the study. AB, JL and SP prepared the reference gas mixtures (RGMs) used for generated SI-traceable working standards based on the dilution of RGMs. PS, MH and MKV prepared the SI-traceable working standards based on air samples, which were certified by AB and MI-G. AA designed and coordinated the development of the VeRDi dilution system, with supervision of CP. For the assessment measurements, ES, SD, TS and RH performed the PTR-ToF-MS measurements and PS, MH, AB and AC performed the TD-GC-FID measurements. AB, JL, CS and MI-G  
1025 carried out the OVOC RGM comparison. MI-G wrote the paper with assistance from all authors, who provided information on instrument description and data. All authors reviewed and approved the latest version of the paper.

**Competing interests**

The contact author has declared that none of the author has any competing interests.

**Acknowledgments**

1030 We acknowledge the technical staff at ACTRIS CiGaS units (IMT Nord Europe, Empa, DWD) and the participating laboratories for their support. Special thanks to the Tropospheric Ozone Precursors Focus Working group for their valuable comments to improve the paper. Utrecht University received support from the Ruisdael Observatory, a scientific infrastructure co-financed by the Dutch Research Council (NOW, grant number 184.034.015).

**Financial support**

1035 This research was performed within the framework of the project 19ENV06 MetClimVOC, which has received funding from the EMPIR programme cofinanced by the Participating States and from the European Union's Horizon 2020 research and innovation programme.

## References

- 1040 Alink, A. and Van Der Veen, A. M. H.: Uncertainty calculations for the preparation of primary gas mixtures Part 1: Gravimetry, *Metrologia*, 37, 641–650, 2000.
- Apel, E. C., Calvert, J. G., Greenberg, J. P., Riemer, D., Zika, R., Kleindienst, T. E., Lonneman, W. A., Fung, K., and Fujita, E.: Generation and validation of oxygenated volatile organic carbon standards for the 1995 Southern Oxidants Study Nashville Intensive, *Journal of Geophysical Research Atmospheres*, 103, 22281–22294, <https://doi.org/10.1029/98JD01383>, 1998.
- 1045 Atkinson, R.: Atmospheric chemistry of VOCs and NO<sub>x</sub>, *Atmos Environ*, 34, 2063–2101, [https://doi.org/10.1016/S1352-2310\(99\)00460-4](https://doi.org/10.1016/S1352-2310(99)00460-4), 2000.
- Bates, K. H., Jacob, D. J., Wang, S., Hornbrook, R. S., Apel, E. C., Kim, M. J., Millet, D. B., Wells, K. C., Chen, X., Brewer, J. F., Ray, E. A., Commane, R., Diskin, G. S., and Wofsy, S. C.: The Global Budget of Atmospheric Methanol: New Constraints on Secondary, Oceanic, and Terrestrial Sources, *Journal of Geophysical Research: Atmospheres*, 126, 1050 <https://doi.org/10.1029/2020JD033439>, 2021.
- De Bièvre, P. and Taylor, P. D. P.: Traceability to the SI of amount-of-substance measurements: From ignoring to realizing, a chemist's view, *Metrologia*, 34, 67–75, <https://doi.org/10.1088/0026-1394/34/1/10>, 1997.
- Boucher, O., Randall, D., Artaxo, P., Bretherton, C., Feingold, G., Forster, P., Kerminen, V.-M., Kondo, Y., Liao, H., Lohmann, U., Rasch, P., Satheesh, S.K., Sherwood, S., Stevens, B., and Zhang, X. Y.: Clouds and aerosols in *Climate Change 2013: The Physical Science Basis. Contribution of Working Group I to the Fifth Assessment Report of the Intergovernmental Panel on Climate Change* (eds Stocker, T.F., Qin, D., Plattner, G.-K., Tignor, M., Allen, S.K., Doschung, J., Nauels, A., Xia, Y., Bex, V., and Midgley, P. M.), Cambridge University Press, 571–657, 1055 <https://doi.org/10.1017/CBO9781107415324.016> (2013).
- Brewer, J. F., Fischer, E. V., Commane, R., Wofsy, S. C., Daube, B. C., Apel, E. C., Hills, A. J., Hornbrook, R. S., Barletta, B., Meinardi, S., Blake, D. R., Ray, E. A., and Ravishankara, A. R.: Evidence for an Oceanic Source of Methyl Ethyl Ketone to the Atmosphere, *Geophys Res Lett*, 47, <https://doi.org/10.1029/2019GL086045>, 2020. 1060
- Brewer, P. J., Brown, R. J. C., Tarasova, O. A., Hall, B., Rhoderick, G. C., and Wielgosz, R. I.: SI traceability and scales for underpinning atmospheric monitoring of greenhouse gases, *Metrologia*, 55, S174–S181, <https://doi.org/10.1088/1681-7575/aad830>, 2018.
- 1065 Brown, A. S., Milton, M. J. T., Brookes, C., Vargha, G. M., Downey, M. L., Uehara, S., Augusto, C. R., Fioravante, A. de L., Sobrinho, D. G., Dias, F., Woo, J. C., Kim, B. M., Kim, J. S., Mace, T., Fükö, J. T., Qiao, H., Guenther, F., Rhoderick, J., Gameson, L., Botha, A., Tshilongo, J., Ntsasa, N. G., Val'ková, M., Durisova, Z., Kustikov, Y., Konopelko, L., Fatina, O.,

and Wessel, R.: Final report on CCQM-K93: Preparative comparison of ethanol in nitrogen, *Metrologia*, 50, 08025–08025, <https://doi.org/10.1088/0026-1394/50/1A/08025>, 2013.

1070 Collins, W. J., Derwent, R. G., Johnson, C. E., and Stevenson, D. S.: The oxidation of organic compounds in the troposphere and their global warming potentials, *Clim Change*, 52, 453–479, <https://doi.org/10.1023/A:1014221225434>, 2002.

Cooper, O. R., Parrish, D. D., Ziemke, J., Balashov, N. V., Cupeiro, M., Galbally, I. E., Gilge, S., Horowitz, L., Jensen, N. R., Lamarque, J. F., Naik, V., Oltmans, S. J., Schwab, J., Shindell, D. T., Thompson, A. M., Thouret, V., Wang, Y., and Zbinden, R. M.: Global distribution and trends of tropospheric ozone: An observation-based review, *Elem Sci Anth*, 2, 000029, <https://doi.org/10.12952/journal.elementa.000029>, 2014.

Coplen, T.B., Holden, N.E., Ding, T., Meijer, H.A.J., Vogl, J., and Zhu, X. The table of standard atomic weights – An exercise in consensus. *Rapid Communication in Mass Spectrometry*, 36, e8864, <https://doi.org/10.1002/rcm.8864>, 2020.

Van Dingenen, R., Dentener, F. J., Raes, F., Krol, M. C., Emberson, L., and Cofala, J.: The global impact of ozone on agricultural crop yields under current and future air quality legislation, *Atmos Environ*, 43, 604–618, <https://doi.org/10.1016/j.atmosenv.2008.10.033>, 2009.

Faiola, C. L., Erickson, M. H., Fricaud, V. L., Jobson, B. T., and Vanreken, T. M.: Quantification of biogenic volatile organic compounds with a flame ionization detector using the effective carbon number concept, *Atmos Meas Tech*, 5, 1911–1923, <https://doi.org/10.5194/amt-5-1911-2012>, 2012.

Fischer, E. V., Jacob, D. J., Millet, D. B., Yantosca, R. M., and Mao, J.: The role of the ocean in the global atmospheric budget of acetone, *Geophys Res Lett*, 39, <https://doi.org/10.1029/2011GL050086>, 2012.

Fischer, E. V., Jacob, D. J., Yantosca, R. M., Sulprizio, M. P., Millet, D. B., Mao, J., Paulot, F., Singh, H. B., Roiger, A., Ries, L., Talbot, R. W., Dzepina, K., and Pandey Deolal, S.: Atmospheric peroxyacetyl nitrate (PAN): A global budget and source attribution, *Atmos Chem Phys*, 14, 2679–2698, <https://doi.org/10.5194/acp-14-2679-2014>, 2014.

Fleming, Z. L., Doherty, R. M., Von Schneidmesser, E., Malley, C. S., Cooper, O. R., Pinto, J. P., Colette, A., Xu, X., Simpson, D., Schultz, M. G., Lefohn, A. S., Hamad, S., Moolla, R., Solberg, S., and Feng, Z.: Tropospheric Ozone Assessment Report: Present-day ozone distribution and trends relevant to human health, *Elementa*, 6, <https://doi.org/10.1525/elementa.273>, 2018.

Galbally, I. E., Schultz, M. G., Buchmann, B., Gilge, S., Guenther, F., Koide, H., Oltmans, S., Patrick, L., Scheel, H.-E., Smit, H., Steinbacher, M., Steinbrecht, W., Tarasova, O., Viallon, J., Volz-Thomas, A., Weber, M., Wielgosz, R., and Zellweger, C.: Guidelines for Continuous Measurement of Ozone in the Troposphere, GAW Report No 209, Publication WMO-No. 1110, WMO, Geneva, 1–76 pp., 2013.

- Gaudel, A., Cooper, O. R., Ancellet, G., Barret, B., Boynard, A., Burrows, J. P., Clerbaux, C., Coheur, P. F., Cuesta, J., Cuevas, E., Doniki, S., Dufour, G., Ebojje, F., Foret, G., Garcia, O., Granados-Muñoz, M. J., Hannigan, J. W., Hase, F., Hassler, B., Huang, G., Hurtmans, D., Jaffe, D., Jones, N., Kalabokas, P., Kerridge, B., Kulawik, S., Latter, B., Leblanc, T., Le Flochmoën, E., Lin, W., Liu, J., Liu, X., Mahieu, E., McClure-Begley, A., Neu, J. L., Osman, M., Palm, M., Petetin, H., Petropavlovskikh, I., Querel, R., Rahpoe, N., Rozanov, A., Schultz, M. G., Schwab, J., Siddans, R., Smale, D., Steinbacher, M., Tanimoto, H., Tarasick, D. W., Thouret, V., Thompson, A. M., Trickl, T., Weatherhead, E., Wespes, C., Worden, H. M., Vigouroux, C., Xu, X., Zeng, G., and Ziemke, J.: Tropospheric Ozone Assessment Report: Present-day distribution and trends of tropospheric ozone relevant to climate and global atmospheric chemistry model evaluation, *Elementa*, 6, <https://doi.org/10.1525/elementa.291>, 2018.
- Goldstein, A. H. and Galbally, I. E.: Known and Unexplored Organic Constituents in the Earth's Atmosphere, *Environ Sci Technol*, 41, 1502–1800, <https://doi.org/10.1021/es072476p>, 2007.
- de Gouw, J. and Warneke, C.: Measurements of volatile organic compounds in the earth's atmosphere using proton-transfer-reaction mass spectrometry, *Mass Spectrom Rev*, 26, 223–257, <https://doi.org/10.1002/mas.20119>, 2007.
- Grenfell, R. J. P., Milton, M. J. T., Harling, A. M., Vargha, G. M., Brookes, C., Quincey, P. G., and Woods, P. T.: Standard mixtures of ambient volatile organic compounds in synthetic and whole air with stable reference values, *Journal of Geophysical Research Atmospheres*, 115, D14302, <https://doi.org/10.1029/2009JD012933>, 2010.
- Güttler, B. and Richter, W.: Traceability of chemical measurement results, *Chimia (Aarau)*, 63, 619–623, <https://doi.org/10.2533/chimia.2009.619>, 2009.
- Hoerger, C. C., Claude, A., Plass-Duelmer, C., Reimann, S., Eckart, E., Steinbrecher, R., Aalto, J., Arduini, J., Bonnaire, N., Cape, J. N., Colomb, A., Connolly, R., Diskova, J., Dumitrean, P., Ehlers, C., Gros, V., Hakola, H., Hill, M., Hopkins, J. R., Jäger, J., Junek, R., Kajos, M. K., Klemp, D., Leuchner, M., Lewis, A. C., Locoge, N., Maione, M., Martin, D., Michl, K., Nemitz, E., O'Doherty, S., Pérez Ballesta, P., Ruuskanen, T. M., Sauvage, S., Schmidbauer, N., Spain, T. G., Straube, E., Vana, M., Vollmer, M. K., Wegener, R., and Wenger, A.: ACTRIS non-methane hydrocarbon intercomparison experiment in Europe to support WMO GAW and EMEP observation networks, *Atmos Meas Tech*, 8, 2715–2736, <https://doi.org/10.5194/amt-8-2715-2015>, 2015.
- Holzinger, R., Joe Acton, W. F., Bloss, W. W., Breitenlechner, M., Crilley, L. L., Dusanter, S., Gonin, M., Gros, V., Keutsch, F. F., Kiendler-Scharr, A., Kramer, L. L., Krechmer, J. J., Languille, B., Locoge, N., Lopez-Hilfiker, F., Materi, D., Moreno, S., Nemitz, E., Quéléver, L. L., Sarda Esteve, R., Sauvage, S., Schallhart, S., Sommariva, R., Tillmann, R., Wedel, S., Worton, D. D., Xu, K., and Zaytsev, A.: Validity and limitations of simple reaction kinetics to calculate concentrations of organic compounds from ion counts in PTR-MS, *Atmos Meas Tech*, 12, 6193–6208, <https://doi.org/10.5194/amt-12-6193-2019>, 2019.



- 1130 Hu, L., Millet, D. B., Mohr, M. J., Wells, K. C., Griffis, T. J., and Helmig, D.: Sources and seasonality of atmospheric methanol based on tall tower measurements in the US Upper Midwest, *Atmos Chem Phys*, 11, 11145–11156, <https://doi.org/10.5194/acp-11-11145-2011>, 2011.
- Iglesias-Suarez, F., Kinnison, D. E., Rap, A., Maycock, A. C., Wild, O., and Young, P. J.: Key drivers of ozone change and its radiative forcing over the 21st century, <https://doi.org/10.5194/acp-18-6121-2018>, 3 May 2018.
- 1135 ISO 6145-10:2002 Gas analysis – Preparation of calibration gas mixtures using dynamic volumetric methods – Part 10: Permeation method, 1<sup>st</sup> edition, International Organization for Standardization (ISO), Geneva, Switzerland, 16 pp., 2002. <https://iso.org/standard/25916.html>, last access: 20 October 2023.
- ISO 6145-4:2004 Gas analysis – Preparation of calibration gas mixtures using dynamic volumetric methods – Part 4: Continuous syringe injection method, 2<sup>nd</sup> edition, International Organization for Standardization (ISO), Geneva, Switzerland, 15 pp., 2004. <https://iso.org/standard/36478.html>, last access: 20 October 2023.
- 1140 ISO 6145-8:2005 Gas analysis – Preparation of calibration gas mixtures using dynamic volumetric methods – Part 8: Diffusion method, 1<sup>st</sup> Edition, International Organization for Standardization (ISO), 19 pp., 2005. <https://iso.org/standard/36480.html>, last access: 20 October 2023.
- ISO 6142-1:2015 Gas analysis – Preparation of calibration gas mixtures – Part 1: Gravimetric method for Class I mixtures, 1<sup>st</sup> edition, International Organization for Standardization (ISO), Geneva, Switzerland, 39 pp., 2015. <https://iso.org/standard/59631.html>, last access: 20 October 2023.
- 1145 ISO 6145-7:2018 Gas analysis – Preparation of calibration gas mixtures using dynamic methods – Part 7: Thermal mass-flow controllers, 3<sup>rd</sup> edition, International Organization for Standardization (ISO), 14 pp., 2018. <https://iso.org/standard/73212.html>, last access: 20 October 2023.
- ISO 19229:2019: Gas analysis – Purity analysis and the treatment of purity data, 2<sup>nd</sup> Edition, International Organization for Standardization (ISO), Geneva, Switzerland, 18 pp., 2019. <https://iso.org/standard/72010.html>, last access: 20 October 2023.
- 1150 Iturrate-Garcia, M., Salameh, T., Schlauri, P., Baldan, A., Vollmer, M.K., Stratigou, E., Dusanter, S., Li, J., Persijn, S., Claude, A., Holzinger, R., Sutour, C., and Reimann, S.: Data from: Towards a high quality in-situ observation network for oxygenated volatile organic compounds (OVOCs) in Europe: transferring traceability to the International System of Units (SI) to the field, Version 1.0.0, Zenodo [data set], <https://doi.org/10.5281/zenodo.14178374>, 2024.
- 1155 Jacob, D. J.: Heterogeneous chemistry and tropospheric ozone, *Atmospheric Environment*, 2131–2159 pp., [https://doi.org/10.1016/S1352-2310\(99\)00462-8](https://doi.org/10.1016/S1352-2310(99)00462-8), 2000.

- JCGM 100:2008 BIPM, IEC, IFCC, ILAC, ISO, IUPAC, IUPAP and OIML. Evaluation of measurement data – Guide to the expression of uncertainty in measurement (GUM). Joint Committee for Guides in Metrology (JCGM), 134 pp., 2008. [https://www.bipm.org/documents/20126/2071204/JCGM\\_100\\_2008\\_E.pdf/cb0ef43f-baa5-11cf-3f85-4dcd86f77bd6](https://www.bipm.org/documents/20126/2071204/JCGM_100_2008_E.pdf/cb0ef43f-baa5-11cf-3f85-4dcd86f77bd6), last access: 20 October 2023.
- 1160 Khan, M. A. H., Cooke, M. C., Utembe, S. R., Archibald, A. T., Maxwell, P., Morris, W. C., Xiao, P., Derwent, R. G., Jenkin, M. E., Percival, C. J., Walsh, R. C., Young, T. D. S., Simmonds, P. G., Nickless, G., O’Doherty, S., and Shallcross, D. E.: A study of global atmospheric budget and distribution of acetone using global atmospheric model STOCHEM-CRI, *Atmos Environ*, 112, 269–277, <https://doi.org/10.1016/j.atmosenv.2015.04.056>, 2015.
- 1165 Laj, P., Lund Myhre, C., Riffault, V., Amiridis, V., Fuchs, H., Eleftheriadis, K., Petäjä, T., Salameh, T., Kivekäs, N., Juurola, E., Saponaro, G., Philippin, S., Cornacchia, C., Alados Arboledas, L., Baars, H., Claude, A., De Mazière, M., Dils, B., Dufresne, M., Evangeliou, N., Favez, O., Fiebig, M., Haeffelin, M., Herrmann, H., Höhler, K., Illmann, N., Kreuter, A., Ludewig, E., Marinou, E., Möhler, O., Mona, L., Murberg, L.E., Nicolae, D., Novelli, A., O’Connor, E., Ohneiser, K., Petracca Altieri, R. M., Picquet-Varrault, B., van Pinxteren, D., Pospichal, B., Putaud, J. P., Reimann, S., Siomos, N., Stachlewska, I., Tillmann, R., Avoudouri, K.A., Wandinger, U., Wiedenshohler, A., Apituley, A., Comerón, A., Gysel-Beer, M., Mihalopoulos, N., Nikolova, N., Pietruczuk, A., Sauvage, S., Sciare, J., Skov, H., Svendby, T., Swietlicki, E., Tonev, D., Vaughan, G., Zdimal, V., Baltensperger, U., Doussin, J.-F., Kulmala, M., Pappalardo, G., Sorvari S. S., and Vana, M.: Aerosol, Clouds and Trace Gases Research Infrastructure – ACTRIS, the European research infrastructure supporting atmospheric science. *Bull Am Meteorol Soc.*, <https://doi.org/10.1175/BAMS-D-23-0064.1>, 2024.
- 1170
- 1175 Legreid, G., Lööv, J. B., Staehelin, J., Hueglin, C., Hill, M., Buchmann, B., Prevot, A. S. H., and Reimann, S.: Oxygenated volatile organic compounds (OVOCs) at an urban background site in Zürich (Europe): Seasonal variation and source allocation, *Atmos Environ*, 41, 8409–8423, <https://doi.org/10.1016/j.atmosenv.2007.07.026>, 2007.
- Lelieveld, J. and Dentener, F. J.: What controls tropospheric ozone?, *Journal of Geophysical Research Atmospheres*, 105, 3531–3551, <https://doi.org/10.1029/1999JD901011>, 2000.
- 1180 Leuenberger, M. C., Schibig, M. F., and Nyfeler, P.: Gas adsorption and desorption effects on cylinders and their importance for long-term gas records, *Atmos Meas Tech*, 8, 5289–5299, <https://doi.org/10.5194/amt-8-5289-2015>, 2015.
- Matschat, R., Richter, S., Vogl, J., and Kipphardt, H.: On the way to SI traceable primary transfer standards for amount of substance measurements in inorganic chemical analysis, *Anal Bioanal Chem*, 415, 3057–3071, <https://doi.org/10.1007/s00216-023-04660-4>, 2023.
- 1185 Miller, W. R., Rhoderick, G. C., and Guenther, F. R.: Investigating adsorption/desorption of carbon dioxide in aluminum compressed gas cylinders, *Anal Chem*, 87, 1957–1962, <https://doi.org/10.1021/ac504351b>, 2015.

- 1190 Millet, D. B., Guenther, A., Siegel, D. A., Nelson, N. B., Singh, H. B., De Gouw, J. A., Warneke, C., Williams, J., Eerdekens, G., Sinha, V., Karl, T., Flocke, F., Apel, E., Riemer, D. D., Palmer, P. I., and Barkley, M.: Atmospheric Chemistry and Physics Global atmospheric budget of acetaldehyde: 3-D model analysis and constraints from in-situ and satellite observations, *Atmos. Chem. Phys.*, 3405–3425 pp., <https://doi.org/10.5194/acp-10-3405-2010>, 2010.
- Mills, G., Pleijel, H., Malley, C. S., Sinha, B., Cooper, O. R., Schultz, M. G., Neufeld, H. S., Simpson, D., Sharps, K., Feng, Z., Gerosa, G., Harmens, H., Kobayashi, K., Saxena, P., Paoletti, E., Sinha, V., and Xu, X.: Tropospheric ozone assessment report: Present-day tropospheric ozone distribution and trends relevant to vegetation, *Elementa*, 6, <https://doi.org/10.1525/elementa.302>, 2018.
- 1195 Monks, P. S., Archibald, A. T., Colette, A., Cooper, O., Coyle, M., Derwent, R., Fowler, D., Granier, C., Law, K. S., Mills, G. E., Stevenson, D. S., Tarasova, O., Thouret, V., Von Schneidmesser, E., Sommariva, R., Wild, O., and Williams, M. L.: Tropospheric ozone and its precursors from the urban to the global scale from air quality to short-lived climate forcer, <https://doi.org/10.5194/acp-15-8889-2015>, 13 August 2015.
- 1200 Pascale, C., Guillevic, M., Ackermann, A., Leuenberger, D., and Niederhauser, B.: Two generators to produce SI-traceable reference gas mixtures for reactive compounds at atmospheric levels, *Meas Sci Technol*, 28, <https://doi.org/10.1088/1361-6501/aa870c>, 2017.
- Persijn, S. T. and Baldan, A.: A new look at the sorption kinetics in reference gas standards, *Meas Sci Technol*, 34, <https://doi.org/10.1088/1361-6501/ace9ee>, 2023.
- 1205 Placet, M.: Emissions of ozone precursors from stationary sources: a critical review, *Atmos Environ*, 34, 2183–2204, [https://doi.org/10.1016/S1352-2310\(99\)00464-1](https://doi.org/10.1016/S1352-2310(99)00464-1), 2000.
- Pugliese, S. C., Murphy, J. G., Geddes, J. A., and Wang, J. M.: The impacts of precursor reduction and meteorology on ground-level ozone in the Greater Toronto Area, *Atmos Chem Phys*, 14, 8197–8207, <https://doi.org/10.5194/acp-14-8197-2014>, 2014.
- 1210 Reimann, S., Wegener, R., Claude, A., and Sauvage, S. Deliverable 3.17. Updated measurement guideline for NO<sub>x</sub> and VOCs. ACTRIS report, 103 pp., [https://actris.eu/sites/default/files/Documents/ACTRIS-2/Deliverables/WP3\\_D3.17\\_M42.pdf](https://actris.eu/sites/default/files/Documents/ACTRIS-2/Deliverables/WP3_D3.17_M42.pdf), 2018.
- Rhoderick, G. C., Cecelski, C. E., Miller, W. R., Worton, D. R., Moreno, S., Brewer, P. J., Viallon, J., Idrees, F., Moussay, P., Kim, Y. D., Kim, D., Lee, S., Baldan, A., and Li, J.: Stability of gaseous volatile organic compounds contained in gas cylinders with different internal wall treatments, *Elementa*, 7, <https://doi.org/10.1525/elementa.366>, 2019.
- 1215 Richter, W.: Recommendations on quantities, symbols and measurement units for publications in ACQUAL, *Accreditation and Quality Assurance*, 12, 497–498, <https://doi.org/10.1007/s00769-007-0273-6>, 2007.

- Seinfeld, J. H., Bretherton, C., Carslaw, K. S., Coe, H., DeMott, P. J., Dunlea, E.J., Feingold, G., Ghan, S., Guenther, A. B., Kahn, R., Kraucunas, I., Kreidenweis, S. M., Molina, M. J., Nenes, A., Penner, J.E., Prather, K. A., Ramanathan, V., Ramaswamy, V., Rasch, P. J., Ravishankara, A. R., Rosenfeld, D., Stephens, G., and Wood, R.: Improving our fundamental understanding of the role of aerosol-cloud interactions in the climate system. *PNAS*, 113, 5781–5790. <https://doi.org/10.1073/pnas.1514043113>, 2016.
- 1220
- Schultz, M. G., Akimoto, H., Bottenheim, J., Buchmann, B., Galbally, I. E., Gilge, S., Helmig, D., Koide, H., Lewis, A. C., Novelli, P. C., Plass-Döhlmer, C., Ryerson, T. B., Steinbacher, M., Steinbrecher, R., Tarasova, O., Tørseth, K., Thouret, V., and Zellweger, C.: The Global Atmosphere Watch reactive gases measurement network, *Elementa*, 3, 000067, 2015.
- 1225
- Schultz, M. G., Schröder, S., Lyapina, O., Cooper, O. R., Galbally, I., Petropavlovskikh, I., Von Schneidemesser, E., Tanimoto, H., Elshorbany, Y., Naja, M., Seguel, R. J., Dauert, U., Eckhardt, P., Feigenspan, S., Fiebig, M., Hjellbrekke, A. G., Hong, Y. D., Kjeld, P. C., Koide, H., Lear, G., Tarasick, D., Ueno, M., Wallasch, M., Baumgardner, D., Chuang, M. T., Gillett, R., Lee, M., Molloy, S., Moolla, R., Wang, T., Sharps, K., Adame, J. A., Ancellet, G., Apadula, F., Artaxo, P., Barlasina, M. E., Bogucka, M., Bonasoni, P., Chang, L., Colomb, A., Cuevas-Agulló, E., Cupeiro, M., Degorska, A., Ding, A., Fröhlich, M., Frolova, M., Gadhavi, H., Gheusi, F., Gilge, S., Gonzalez, M. Y., Gros, V., Hamad, S. H., Helmig, D., Henriques, D., Hermansen, O., Holla, R., Hueber, J., Im, U., Jaffe, D. A., Komala, N., Kubistin, D., Lam, K. S., Laurila, T., Lee, H., Levy, I., Mazzoleni, C., Mazzoleni, L. R., McClure-Begley, A., Mohamad, M., Murovec, M., Navarro-Comas, M., Nicodim, F., Parrish, D., Read, K. A., Reid, N., Ries, L., Saxena, P., Schwab, J. J., Scorgie, Y., Senik, I., Simmonds, P., Sinha, V., Skorokhod, A. I., Spain, G., Spangl, W., Spoor, R., Springston, S. R., Steer, K., Steinbacher, M., Suharguniyawan, E., Torre, P., Trickl, T., Weili, L., Weller, R., Xiaobin, X., Xue, L., and Zhiqiang, M.: Tropospheric Ozone Assessment Report: Database and metrics data of global surface ozone observations, *Elementa*, 5, <https://doi.org/10.1525/elementa.244>, 2017.
- 1230
- 1235
- Shao, M., Lu, S., Liu, Y., Xie, X., Chang, C., Huang, S., and Chen, Z.: Volatile organic compounds measured in summer in Beijing and their role in ground-level ozone formation, *Journal of Geophysical Research Atmospheres*, 114, <https://doi.org/10.1029/2008JD010863>, 2009.
- 1240
- Shrivastava, M., Cappa, C. D., Fan, J., Goldstein, A. H., Guenther, A. B., Jimenez, J. L., Kuang, C., Laskin, A., Martin, S. T., Ng, N. L., Petaja, T., Pierce, J. R., Rasch, P. J., Roldin, P., Seinfeld, J. H., Shilling, J., Smith, J. N., Thornton, J. A., Volkamer, R., Wang, J., Worsnop, D. R., Zaveri, R. A., Zelenyuk, A., and Zhang, Q.: Recent advances in understanding secondary organic aerosol: Implications for global climate forcing, *Rev Geophys*, 55, 509–559, <https://doi.org/10.1002/2016RG000540>, 2017.
- 1245
- Simon, H., Reff, A., Wells, B., Xing, J., and Frank, N.: Ozone trends across the United States over a period of decreasing NO<sub>x</sub> and VOC emissions, *Environ Sci Technol*, 49, 186–195, <https://doi.org/10.1021/es504514z>, 2015.

- Simon, L., Gros, V., Petit, J. E., Truong, F., Sarda-Estève, R., Kalalian, C., Baudic, A., Marchand, C., and Favez, O.: Two years of volatile organic compound online in situ measurements at the Site Instrumental de Recherche par Télédétection Atmosphérique (Paris region, France) using proton-transfer-reaction mass spectrometry, *Earth Syst Sci Data*, 15, 1947–1968, <https://doi.org/10.5194/essd-15-1947-2023>, 2023.
- 1250
- Sternberg, J. C., Gallaway, W. S., and Jones, D. T. L.: The mechanism of response of flame ionization detectors, in: *Gas Chromatography: Third International Symposium Held Under the Auspices of the Analysis Instrumentation Division of the Instrument Society of America*, edited by: Brenner, N., Callen, J. E., and Weiss, M. D., Academic Press, New York and London, 231–267, 1962.
- 1255
- Stohl, A., Bonasoni, P., Cristofanelli, P., Collins, W., Feichter, J., Frank, A., Forster, C., Gerasopoulos, E., Gäggeler, H., James, P., Kentarchos, T., Kromp-Kolb, H., Krüger, B., Land, C., Meloen, J., Papayannis, A., Priller, A., Seibert, P., Sprenger, M., Roelofs, G. J., Scheel, H. E., Schnabel, C., Siegmund, P., Tobler, L., Trickl, T., Wernli, H., Wirth, V., Zanis, P., and Zerefos, C.: Stratosphere-troposphere exchange: A review, and what we have learned from STACCATO, *Journal of Geophysical Research Atmospheres*, 108, <https://doi.org/10.1029/2002jd002490>, 2003.
- 1260
- Szopa, S., Naik, V., Ahikary, B., Artaxo, P., Berntsen, T., Collins, W., Fuzzi, S., Gallardo, L., Kiendler-Scharr, A., Kimont, Z., Liao, H., Unger, N., and Zanis, P.: Short-lived Climate Forcers, in: *Climate Change 2021 – The Physical Science Basis. Contribution of Working Group I to the Sixth Assessment Report of the Intergovernmental Panel on Climate Change*, Cambridge University Press, 817–922, <https://doi.org/10.1017/9781009157896.008>, 2023.
- 1265
- Tan, Z., Lu, K., Hofzumahaus, A., Fuchs, H., Bohn, B., Holland, F., Liu, Y., Rohrer, F., Shao, M., Sun, K., Wu, Y., Zeng, L., Zhang, Y., Zou, Q., Kiendler-Scharr, A., Wahner, A., and Zhang, Y.: Experimental budgets of OH, HO<sub>2</sub>, and RO<sub>2</sub> radicals and implications for ozone formation in the Pearl River Delta in China 2014, *Atmos Chem Phys*, 19, 7129–7150, <https://doi.org/10.5194/acp-19-7129-2019>, 2019.
- 1270
- Tarasick, D., Galbally, I. E., Cooper, O. R., Schultz, M. G., Ancellet, G., Leblanc, T., Wallington, T. J., Ziemke, J., Liu, X., Steinbacher, M., Staehelin, J., Vigouroux, C., Hannigan, J. W., García, O., Foret, G., Zanis, P., Weatherhead, E., Petropavlovskikh, I., Worden, H., Osman, M., Liu, J., Chang, K. L., Gaudel, A., Lin, M., Granados-Muñoz, M., Thompson, A. M., Oltmans, S. J., Cuesta, J., Dufour, G., Thouret, V., Hassler, B., Trickl, T., and Neu, J. L.: Tropospheric ozone assessment report: Tropospheric ozone from 1877 to 2016, observed levels, trends and uncertainties, <https://doi.org/10.1525/elementa.376>, 2019.
- 1275
- van der Veen, A.M.H, Meija, J., Possolo, A., Hibbert, D.B.: Interpretation and use of standard atomic weights (IUPAC Technical Report), *Pure Appl Chem*, 93, 629–646, <https://doi.org/10.1515/pac-2017-1002>, 2021.
- Volkamer, R., Sheehy, P., Molina, L. T., and Molina, M. J.: Oxidative capacity of the Mexico City atmosphere-Part 1: A radical source perspective, *Atmos Chem Phys*, 10, 6969–6991, <https://doi.org/10.5194/acp-10-6969-2010>, 2010.

- 1280 Wang, S., Hornbrook, R. S., Hills, A., Emmons, L. K., Tilmes, S., Lamarque, J. F., Jimenez, J. L., Campuzano-Jost, P., Nault,  
B. A., Crouse, J. D., Wennberg, P. O., Kim, M., Allen, H., Ryerson, T. B., Thompson, C. R., Peischl, J., Moore, F., Nance,  
D., Hall, B., Elkins, J., Tanner, D., Huey, L. G., Hall, S. R., Ullmann, K., Orlando, J. J., Tyndall, G. S., Flocke, F. M., Ray,  
E., Hanisco, T. F., Wolfe, G. M., St. Clair, J., Commane, R., Daube, B., Barletta, B., Blake, D. R., Weinzierl, B., Dollner,  
M., Conley, A., Vitt, F., Wofsy, S. C., Riemer, D. D., and Apel, E. C.: Atmospheric Acetaldehyde: Importance of Air-Sea  
1285 Exchange and a Missing Source in the Remote Troposphere, *Geophys Res Lett*, 46, 5601–5613,  
<https://doi.org/10.1029/2019GL082034>, 2019.
- Wild, O.: Atmospheric Chemistry and Physics Modelling the global tropospheric ozone budget: exploring the variability in  
current models, *Atmos Chem Phys*, <https://doi.org/10.5194/acp-7-2643-2007>, 2007.
- WMO-BIPM: Metrology for Climate Action, Instruments and Observing Methods Report No. 142, Geneva, 88 pp., 2023.  
<https://library.wmo.int/idurl/4/66028>, last access: 25 January 2024.
- 1290 Worton, D. R., Moreno, S., Brewer, P. J., Li, J., Baldan, A., and van der Veen, A. M. H.: Bilateral comparison of primary  
reference materials (PRMs) containing methanol, ethanol and acetone in nitrogen, *Accreditation and Quality Assurance*,  
27, 265–274, <https://doi.org/10.1007/s00769-022-01513-y>, 2022.
- Worton, D. R., Moreno, S., O’Daly, K., and Holzinger, R.: Development of an International System of Units (SI)-traceable  
transmission curve reference material to improve the quantitation and comparability of proton-transfer-reaction mass-  
1295 spectrometry measurements, *Atmos Meas Tech*, 16, 1061–1072, <https://doi.org/10.5194/amt-16-1061-2023>, 2023.
- Wu, C., Wang, C., Wang, S., Wang, W., Yuan, B., Qi, J., Wang, B., Wang, H., Wang, C., Song, W., Wang, X., Hu, W., Lou,  
S., Ye, C., Peng, Y., Wang, Z., Huangfu, Y., Xie, Y., Zhu, M., Zheng, J., Wang, X., Jiang, B., Zhang, Z., and Shao, M.:  
Measurement report: Important contributions of oxygenated compounds to emissions and chemistry of volatile organic  
compounds in urban air, *Atmos Chem Phys*, 20, 14769–14785, <https://doi.org/10.5194/acp-20-14769-2020>, 2020.
- 1300 Xue, L. K., Wang, T., Gao, J., Ding, A. J., Zhou, X. H., Blake, D. R., Wang, X. F., Saunders, S. M., Fan, S. J., Zuo, H. C.,  
Zhang, Q. Z., and Wang, W. X.: Ground-level ozone in four Chinese cities: Precursors, regional transport and  
heterogeneous processes, *Atmos Chem Phys*, 14, 13175–13188, <https://doi.org/10.5194/acp-14-13175-2014>, 2014.
- Yang, M., Nightingale, P.D., Beale, R., Liss, P.S., Blomquist, B., and Fairall, C.: Atmospheric deposition of methanol over  
the Atlantic Ocean, *PNAS*, 110, 20034–20039, <https://doi.org/10.1073/pnas.1317840110>.
- 1305 Yang, Y., Shao, M., Wang, X., Nölscher, A. C., Kessel, S., Guenther, A., and Williams, J.: Towards a quantitative  
understanding of total OH reactivity: A review, *Atmos Environ*, 134, 147–161,  
<https://doi.org/10.1016/j.atmosenv.2016.03.010>, 2016.

- Young, P. J., Naik, V., Fiore, A. M., Gaudel, A., Guo, J., Lin, M. Y., Neu, J. L., Parrish, D. D., Rieder, H. E., Schnell, J. L., Tilmes, S., Wild, O., Zhang, L., Ziemke, J., Brandt, J., Delcloo, A., Doherty, R. M., Geels, C., Hegglin, M. I., Hu, L., Im, U., Kumar, R., Luhar, A., Murray, L., Plummer, D., Rodriguez, J., Saiz-Lopez, A., Schultz, M. G., Woodhouse, M. T., and Zeng, G.: Tropospheric Ozone Assessment Report: Assessment of global-scale model performance for global and regional ozone distributions, variability, and trends, *Elem Sci Anth* 6: 10, 49 pp, <https://doi.org/10.1525/elementa.265>, 2018.
- Zborowska, A. G., MacInnis, C. Y., Ye, C. Z., and Osthoff, H. D.: On the photolysis branching ratio of methyl ethyl ketone, *Atmos Environ*, 254, 118383, <https://doi.org/10.1016/j.atmosenv.2021.118383>, 2021.
- 1315 Zhang, H., Wu, S., Huang, Y., and Wang, Y.: Effects of stratospheric ozone recovery on photochemistry and ozone air quality in the troposphere, *Atmos Chem Phys*, 14, 4079–4086, <https://doi.org/10.5194/acp-14-4079-2014>, 2014.